

Final Contract Report

Refining the Conceptual Model for Flow in the Edwards Aquifer—Characterizing the
Role of Fractures and Conduits in the Balcones Fault Zone Segment

Susan Hovorka, Thandar Phu, J. P. Nicot, Adrien Lindley

Bureau of Economic Geology
Scott W. Tinker, Director
John A. and Katherine G. Jackson School of Geosciences
The University of Texas at Austin

January 16, 2004

ABSTRACT

The Balcones Fault Zone Edwards aquifer of South Texas exhibits multimodal permeability. High matrix porosity and permeability are overshadowed by high permeability developed in structurally influenced karstic conduit systems. High permeability is developed in the confined part of the aquifer at depths greater than 4,000 feet below sea level, as well as in the unconfined zone. Optimization of use of this heavily subscribed aquifer requires accurate quantification and realistic mapping of the relationships between the limestone matrix, which stores most of the water, and the conduit system, which transmits water into, through, and out of the aquifer. This balance between storage and drainage is a key variable needed for predicting sustainability of flow during periods of low recharge and heavy use.

The purpose of this study is to interpret and integrate a selection of the existing diverse data to better characterize the conduit system. Data sets selected to feed into this interpretation include (1) water-level data, (2) structural information, (3) cave maps, (4) existing water-chemistry data, and (5) well hydrographs. It is intended that analysis of the existing data will supply hypotheses that will then be tested using field-based follow-up studies. These might include injected tracers; high frequency, closely spaced water level monitoring; conductivity monitoring; and well testing to better define flow systems.

A regionally extensive system of high-permeability zones is defined by broad troughs in the potentiometric surface in the confined zone. Indications of connections of the confined aquifer to the recharge zone are weakly defined by troughs in the available water-level data. Intersection of the Edwards/Trinity merged potentiometric surface maps with base Edwards structure maps to show that the Edwards Formation is saturated over only a part of the Edwards outcrop zone. This fact suggests that recharge flows through the Edwards into the upper beds of the underlying Glen Rose Formation before returning to the Edwards. Steep gradients of 100 ft/mi are mapped where flow crosses between the Glen Rose and the Edwards Formations, showing that the cross-formational flowpaths are much less transmissive than those in the Edwards confined zone. Spring discharge at the Edwards-Glen Rose contact suggests that perched water tables or flood-stage perched conduits might have a significant role in transmitting water through the recharge zone.

Cave maps show a persistent overprint of vadose-zone karst development, forming near-vertical shafts; however, in the horizontal segments, cave elongation shows that about half the caves are elongated along the principal fault direction. This orientation documents the role of opening-mode fractures parallel to the Balcones Fault Zone trends in controlling permeability. The other half of the horizontally elongated caves trend in other directions, reflecting multiple fracture systems in this structurally complex system. Local gradient toward a local discharge point is interpreted to be a possible contribution to elongations of some cave patterns.

Water chemistry from Texas Water Development Board (TWDB) files is used as an indicator of flowpath geometry. High-salinity water (>3000 mg/L total dissolved solids [TDS]) indicative of long residence times is found in the deep part of the Edwards aquifer and in parts of the Glen Rose (Trinity) aquifer. These areas are therefore interpreted as regions bypassed by low-TDS recharge water moving through conduits.

Other Trinity samples have salinities in the same range as that of average Edwards water (200 to 500 mg/L) and may indicate faster flowpaths that communicate from the Trinity to the Edwards and from the Edwards recharge zone through the Trinity and back into the Edwards. About 5% of the Edwards waters in the confined Edwards are strongly undersaturated with respect to calcite, interpreted as an indicator of rapid conduit flow that has limited reactions between rock and water. Undersaturated samples are not strongly clustered in the major conduits zones defined by troughs in the potentiometric surface, suggesting that a network of conduits is active, with groundwater velocities adequate to impact chemistries. Samples with reported high (more than 30 mg/L) nitrate in the confined aquifer are tentatively interpreted as indicators of fast flowpaths from surface sources of nitrate; however, well leakage and sample contamination are alternative explanations.

Separation of representative well hydrographs recession curves shows variability in the ratio of matrix to fracture storativity. However, strong rapid drainage characteristic of conduits was not observed in the small population of hydrographs analyzed.

TABLE OF CONTENTS

Abstract	i
Introduction	1
Evolution of the Edwards aquifer as a karst flow system	1
Evidence of the karstic properties of the Edwards aquifer	6
Purpose of this study	11
Methods	11
Water-level data	11
Structural mapping and calculation of saturated thickness	14
Analysis of cave maps	14
Water chemistry	15
Well hydrograph separation	15
Results	16
Water-level mapping	19
Intersection of structure and water level	19
Cave map analysis	25
Water quality	29
Analysis of hydrographs	35
Discussion	39
Steep gradients between the confined and unconfined Edwards	40
Trends and variations in the unconfined Edwards	44
Follow-up recommendations	46
Acknowledgments	49
References cited	50

Figures

1. Geologic setting of the South Central Edwards aquifer: depositional and postdepositional elements	3
2. Stratigraphy of the Edwards Group and associated units, focusing on stratigraphic nomenclature used in this study	4
3. Surface-water capture by eastward-flowing streams has created gradients that permitted groundwater capture and diversion to major springs	5
4. Representative karst landforms in the Edwards outcrop zone	7
5. Information about conduit geometry from the Barton Springs Edwards aquifer	9
6. Variograms from kriged water levels	13
7. Low-stage pseudosynoptic	20
8. Intermediate-stage pseudosynoptic	21
9. High-stage pseudosynoptic	22
10. Gridded provisional synoptic data from October 1999	23
11. Water-level change shown by subtracting low from high pseudosynoptic	24
12. Saturated thickness of the Edwards Formation	26
13. Cumulative frequency of the maximum distance in map view of the edge of the mapped cave “footprint” from the entrance	28
14. Distribution of caves analyzed	28
15. TDS in ppm from the TWDB water quality database	30

16. Relative gypsum saturation, from “saturated near 1” to “undersaturation” plotted on the saturated-thickness base	32
17. Calcite saturation, from “saturated near 1” to “undersaturation” plotted on saturated-thickness base	33
18. NO ₃ concentration (ppm) plotted on the saturated-thickness base	34
19. Location of wells selected for hydrograph separation	35
20. Well hydrograph for 68-28-519.....	36
21. Well hydrograph for 68-28-202.....	36
22. Well hydrograph for the SAWS Fish Hatchery # 1 well, 67-09-113, showing comparison of the hydrograph with several rainfall events and a detailed recession separation	38
23. Well hydrograph separation for SAWS Tricounty #3 68-31-511	39
24. Interpreted low-pseudosynoptic water levels with fault patterns superimposed.....	41
25. Conduit indicators and interpreted axes of persistent troughs in the pseudosynoptic potentiometric surface maps	42
26. Schematic cross section of the transition from the unconfined to confined Edwards in the eastern and central parts of the aquifer	43
27. Suggested detailed study areas	47

INTRODUCTION

Evolution of the Edwards aquifer as a karst flow system

The south-central section (fig. 1) of the regionally extensive Edwards aquifer is developed in 450- to 900-ft-thick Lower Cretaceous (Albian) platform carbonates (Hovorka and others, 1996). Original sediments composed of aragonite, calcite, dolomite, and gypsum have been extensively replaced by calcite within the aquifer and are in the process of forming a highly porous and strongly heterogeneous limestone rock. Hydrologically significant heterogeneities within this rock include variable rock fabrics and structural features. Variable rock fabrics include lateral and vertical variation of depositional facies character in response to Cretaceous depositional processes, which has formed beds of varying solubility and mechanical properties. These variable rock fabrics are stacked to form regionally extensive stratigraphic intervals having distinctive rock properties that are mapped as formations and hydrostratigraphic members. Major stratigraphic units referred to in this paper include the Kainer and Person Formations of the San Marcos Platform, Devils River Formation of the San Marcos Platform margin, and West Nueces, McKnight, and Salmon Peak Formations of the Maverick Basin (figs. 1a and 2). Syndepositional karst was developed at the top of and possibly within the Edwards Group on the San Marcos Platform, and this karst has created a zone of high permeability of unknown continuity at the top of the Edwards Formation (Maclay 1995; Hovorka and others, 1998, their fig. 29). Regional doming and intrusion of Upper Cretaceous mafic igneous bodies through the Edwards Group in the Uvalde Uplift created additional complexity in this part of the aquifer (fig. 1b). Extensional down-to-the-coast faulting forming the Balcones Fault system overprinted earlier-formed heterogeneity. Faulting had a critical role in aquifer evolution because it (1) increased permeability by forming fracture networks and (2) greatly increased hydrologic gradient by uplift of the base of the Edwards Group to elevations greater than 1,500 ft above sea level in the west part of the aquifer, whereas at the maximum downdip extent of the freshwater aquifer the top Edwards is at 3,400 ft below sea level (fig. 1b).

Introduction of freshwater into this heterogeneous and highly permeable carbonate rock created an extensive aquifer, which in turn modified the rock properties by the self-reinforcing mechanisms of preferential flow through larger aperture pores and preferential dissolution in zones of higher flow, forming interconnected large dissolved conduits (for details of this process, see Palmer, 1991). Several significant factors are recognized that control karstic dissolution. One factor is groundwater piracy that has caused diversion of recharge from the west to discharge points at springs in the east and north. Woodruff and Abbott (1986) noted the asymmetry of surface-water drainage gradients, showing capture toward the east as surface streams with eastward flow directions, such as the Colorado-Llano, Pedernales, Blanco, and Guadalupe, have captured the headwaters of southward-draining streams, such as the West Nueces, Frio, Sabinal and Medina (fig. 3). Greater downward incision of east-flowing streams created low points in the Edwards flow system. Capture of local discharge and diversion of flow along higher permeability heterogeneities in the Edwards Group toward these low points has resulted in integration of the entire aquifer to discharge at the high-volume Comal, San Marcos, and Barton Springs.

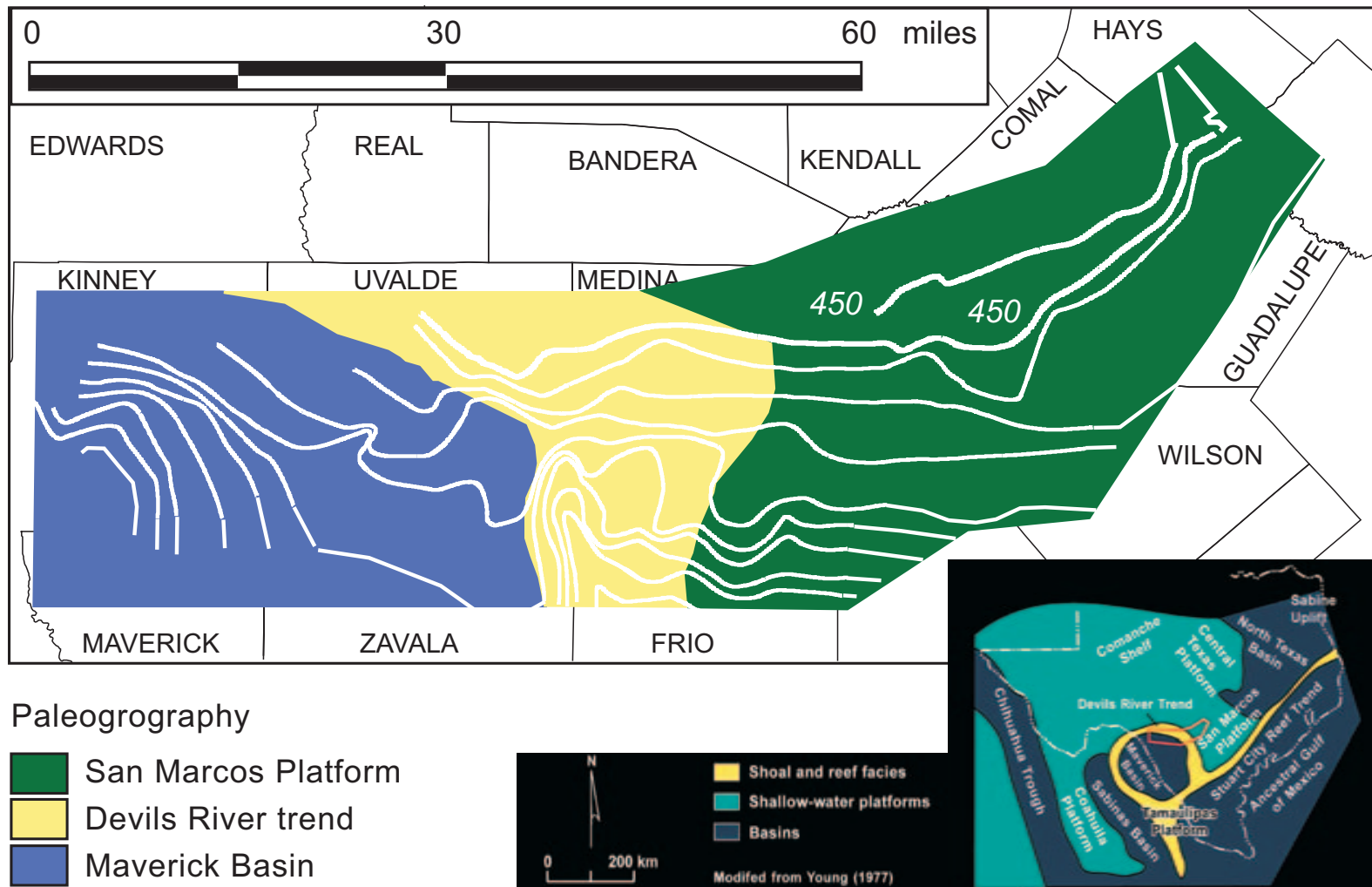


Figure 1. Geologic setting of the South Central (Balcones Fault Zone) Edwards aquifer (a) depositional elements: isopach (modified from Hovorka and others, 1996), paleogeography (modified from Rose, 1972 and Young, 1977).

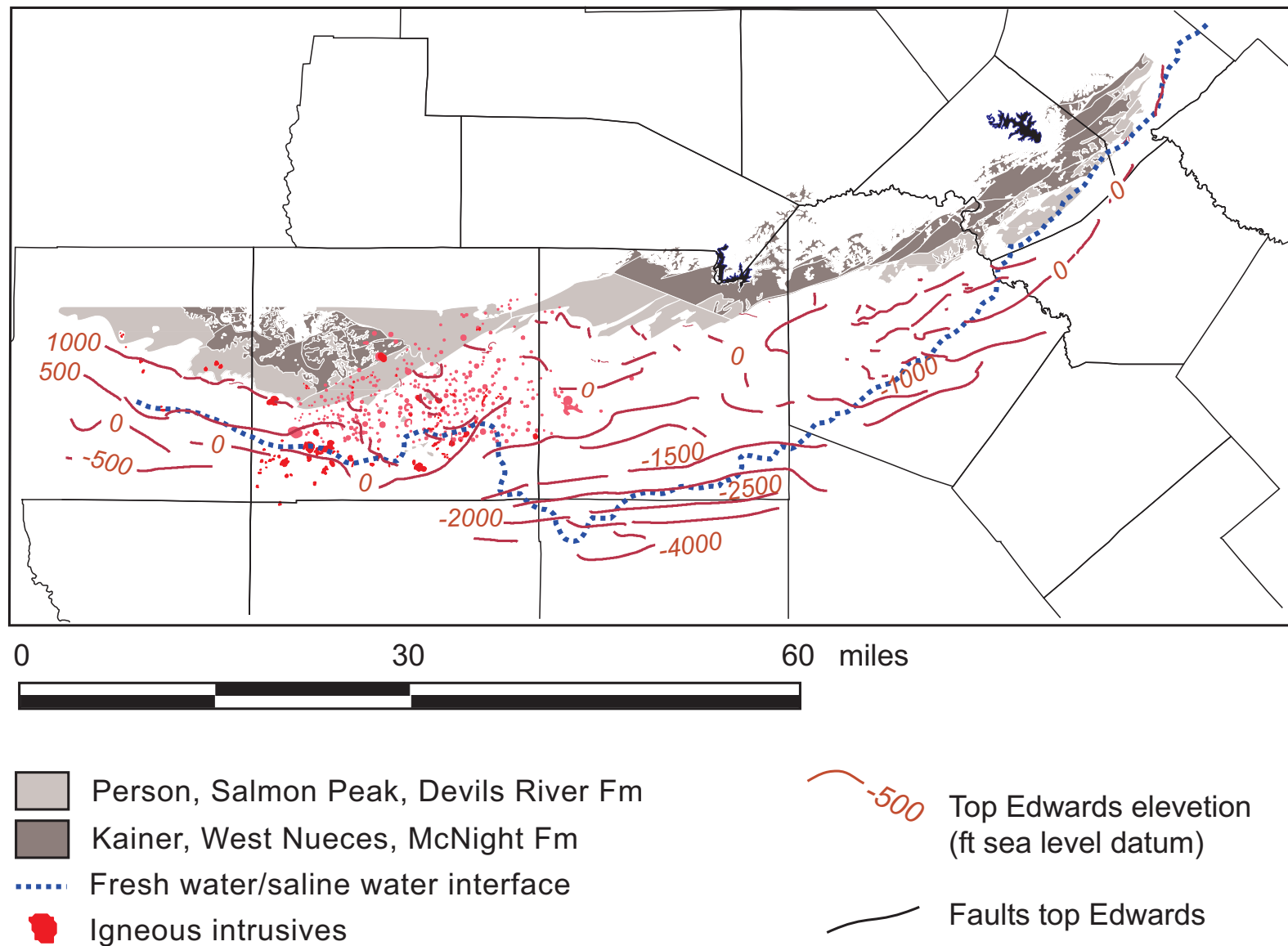


Figure 1. Geologic setting of the South Central (Balcones Fault Zone) Edwards aquifer (b) postdepositional elements: intrusives (Geologic Atlas of Texas and Smith and others, 2002) Uvalde Uplift, current groundwater divides, and maximum downdip extent of freshwater (compiled from Schultz, 1992, 1993, 1994; digitized by USGS).

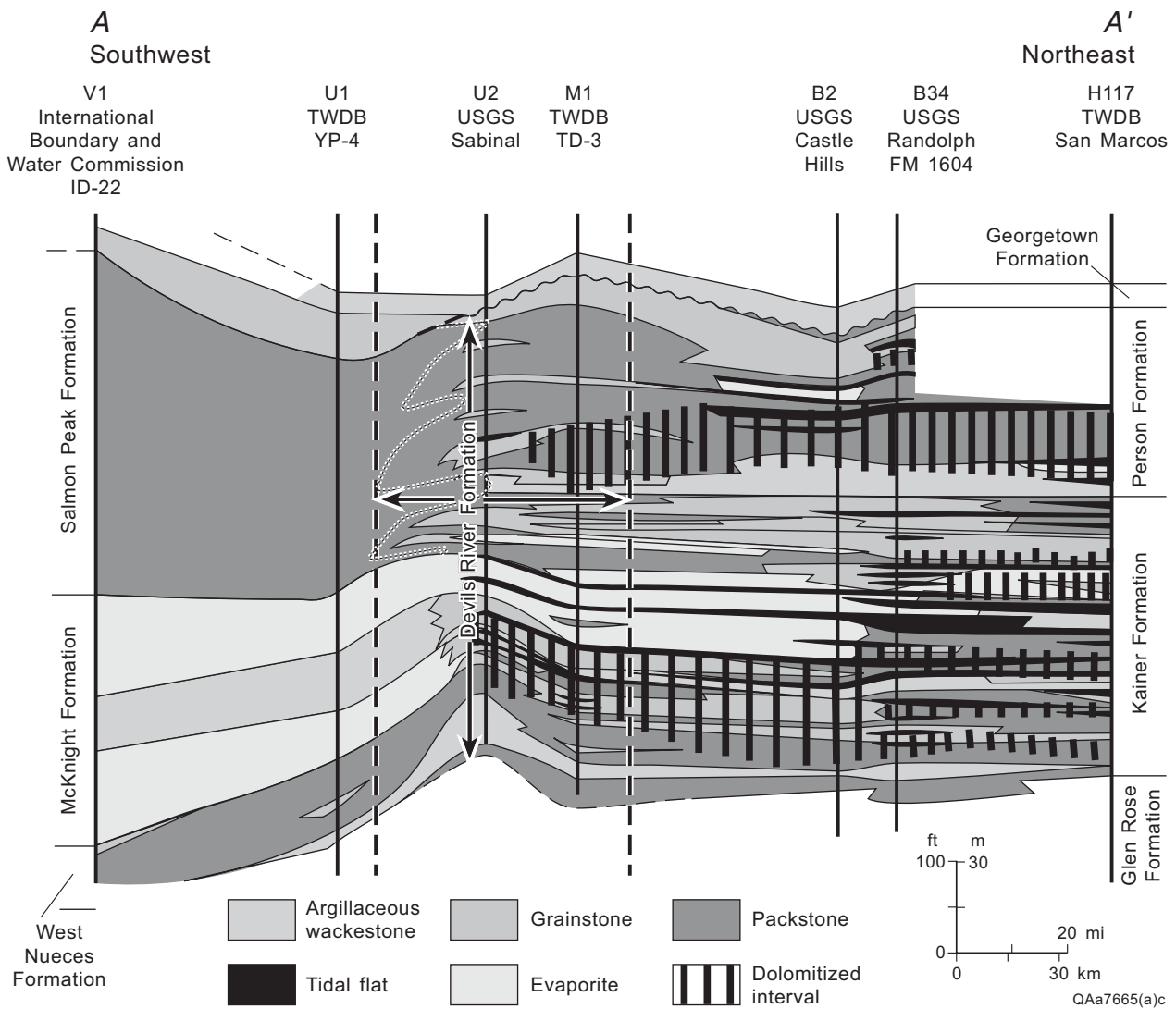


Figure 2. Stratigraphy of the Edwards Group and associated units, focusing on stratigraphic nomenclature used in this study. (From Hovorka and others, 1998.)

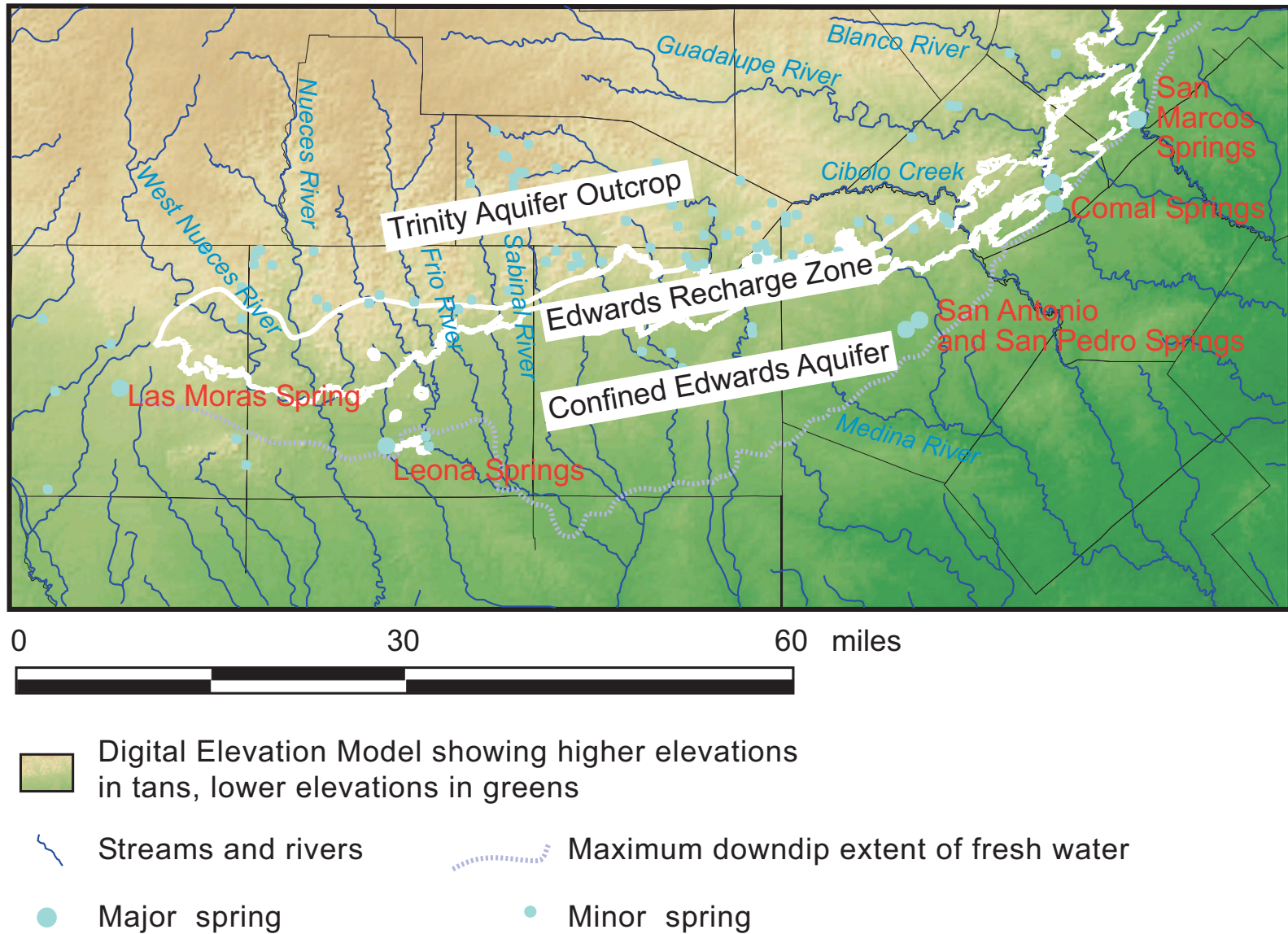


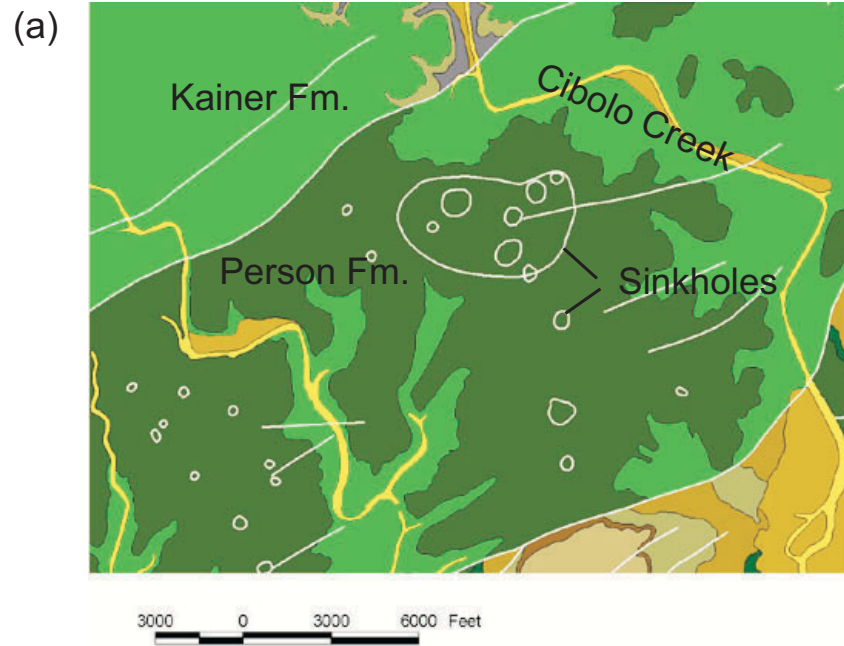
Figure 3. Surface-water capture by eastward-flowing streams has created gradients that permitted groundwater capture and diversion to major springs. Digital elevation model from TNRIS data processed by J. Andrews. Major aquifer recharge zones (TWDB digital data) are superimposed, showing nomenclature applied to regional aquifers. Minor springs are excerpted from USGS and TWDB digital files.

The other factor influencing karst development is dissolution at depth. Undersaturation with respect to dolomite is modeled as a result of mixing low salinity calcium bicarbonate waters in the Edwards aquifer with high salinity calcium sulfate water (Deike, 1990). Petrographic and hydrologic observations provide evidence that mixing-zone dissolution near the interface between fresh and saline water has created high porosity and high permeability preferentially focused where dolomite has been dissolved (Hovorka and others, 1998). Similar deep karst created by upwelling high sulfide water has been documented worldwide (Palmer, 1991; Klimchouk and others, 2000).

Evidence of the karstic properties of the Edwards aquifer from previous work

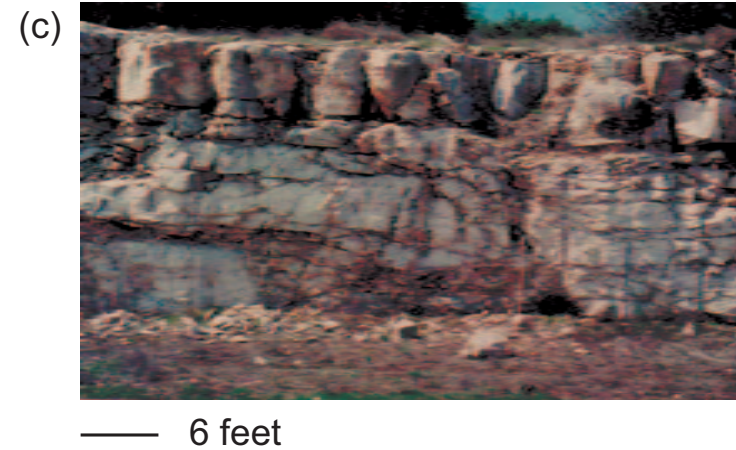
Evidence of the karstic nature of the Edwards aquifer is abundant and diverse and includes outcrop evidence, subsurface data, biologic data, and hydrologic evidence. In outcrop, karst landforms are characteristic of the Edwards Group. Karst landforms include large (up to 1 mi across, but more typically tens to hundreds of feet across) shallow, internally drained depressions (fig. 4a); swallets in creek bottoms; and small upland features such as sinkholes and solution-enlarged fractures. An in-progress inventory in part of the Barton Springs Edwards aquifer recharge zone south of Austin has identified nearly 1,000 karst features in a 40-mi² area on the Edwards outcrop. This inventory is based on compilation of geologic assessment submitted to the Texas Commission on Environmental Quality as part of the water-pollution abatement plan (WPAP) process and an inventory under way by Nico Hauwert for the City of Austin. Inspection of representative geologic assessments of karst features in the Edwards outcrop of the south-central section of the Edwards aquifer suggests that karst-feature density in this segment of the Edwards outcrop is similar to that of the Barton Springs region, although the density has not been quantified. Figure 4b, c shows a typical cave and fracture development in outcrop. More than 400 caves have been inventoried in the Edwards outcrop (Veni, 1988; Elliott and Veni, 1994) and several hundred of them have been mapped and data archived with the Texas Speleological Survey (TSS) (fig. 4d). Caves provide localized access to the deeper parts of the unconfined aquifer, including a few caves where reconnaissance of a flowpath connecting the surface with the saturated section is possible. Wermund and others (1978) documented the alignment of mapped cave passages with lineaments in both the Edwards and Glen Rose Formations, documenting as well the role of structural fabrics in focusing dissolution.

Outcrops provide important information about the origins, dimensions, and distribution of caves; solution-enlarged fractures; and solution along bedding plains. In a previous study (Hovorka and others, 1998), photomosaics were prepared of vertical roadcut outcrops, and the geometry of fractures and solution-enlarged karst features were digitized and quantified in the field and on photographs. In two-dimensional cross section, karst features make up 1 to 5% of the area of the outcrop. Solution enlargement preferentially developed where faults and fractures intersect solution-prone beds. Larger features are preferentially observed in the brecciated zones near small faults. Vertical conduits, some filled with red terra rosa sediments, are observed in some outcrops. These are attributed to a vadose stage of karst evolution postdating and overprinting features developed in the saturated zone.



(b)

6 feet



(d)

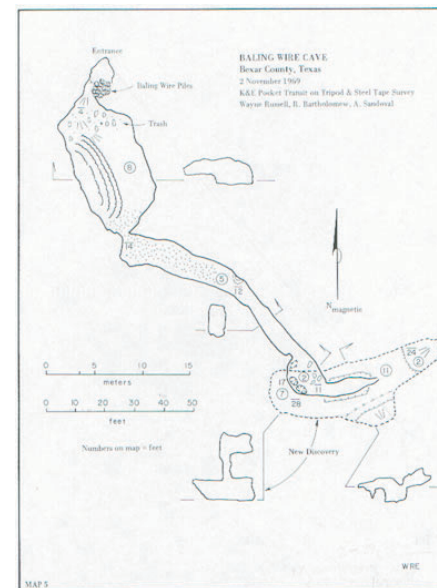


Figure 4. Representative karst landforms in the Edwards outcrop zone. (a) Closed depression on the Person Formation south of Cibolo Creek in northeastern Bexar County; (b) cave opened (and partly consumed) by highway excavation, south loop 620 Comal County; (c) typical expression of fractures, solution-enlarged fractures, and small conduits in outcrop, Stone Oak Parkway, Bexar County; and (d) representative cave map, Baling Wire cave, Bexar County (reproduced from Veni, 1988, p. 59).

Although deep conduits have not been entered by humans, the existence of karst in the deep-subsurface saturated zone is known from borehole televiewer images of caves and solution-enlarged fractures, cave textures and sediments recovered in cores, bit drops during well construction, and oversized caliper logs and off-scale porosity logs. During a previous study (Hovorka and others, 1996), we analyzed porosity of the Edwards Formation using wireline logs. These logs showed significant areas of coincidence between very high porosity and enlarged or off-scale caliper. Some large-scale caliper excursions may be artifacts, such as over-enlarged borehole in weak rocks (especially in the Salmon Peak Formation of the west part of the area), or drilling-induced borehole breakout; however, many oversized boreholes are a result of the borehole intersecting a cave or solution-enlarged bedding plane or fracture. This evidence of karst is found throughout the Edwards Group and is not focused in any particular structural or stratigraphic setting.

Cave biology is a growing research area that will contribute to developing an understanding of connectivity in karst flow systems. A diverse macrofauna adapted to subterranean conditions, including unique species of blind catfish, have been recovered from Edwards wells, demonstrating the existence of adequate habitat to support these species (Longley, 1986). Krejca (2002) used biologic diversity to infer connectivity of Edwards karst systems.

Hydrologic evidence of the nature of karst in the Edwards aquifer is abundant and growing, although additional analysis is needed to quantify flow through this heterogeneous and dynamic system. The principal evidence of karst flow is the heterogeneous and rapidly responsive nature of water-level variation. Water levels in the aquifer and discharge at springs rise rapidly after rainfall and then decline at a variable rate, showing drainage from both conduits and matrix (Paul Hsieh, verbal communication, 2002). Wells close together can have different responses to a single recharge pulse, the Shavano Park monitoring wells (Johnson and other, 2002), for example. Hovorka and others (1998) and Mace and Hovorka (2000) identified eight orders of magnitude variation in hydraulic conductivity with a variogram nugget of 10 mi, showing a high degree of heterogeneity between closely spaced wells. About 15 percent of wells have no measured drawdown during the specific capacity test, showing that hydraulic conductivity of the aquifer is higher than that of the pump-well system. Spring response to rainfall is rapid, occurring within 11 days at Comal Springs and 9 days at San Marcos Springs (Tomasko and others, 2001).

Mapping hydraulic conductivity (Hovorka and others, 1998) shows a strong trend toward high values in the deep confined aquifer compared with those of the unconfined and shallow semiconfined system. A similar trend of porosity increase with depth that crosscuts the depositional trends is noted, supporting an interpretation of enhanced dissolution processes by mixing of saline deep- and freshwaters. Further interpretation of quantitative outcrop and well-test data by Hulihan and others (2000) assessed the connectivity of karst. This assessment modeled the hydraulic conductivity of measured matrix, fractures, and conduits using simplified assumptions about the connectivity of the system. They concluded that Edwards wells having measured hydraulic conductivity are best modeled using a permeability distribution represented by fractures with a maximum apertures in the millimeter range. Although conduits with

apertures in the centimeter to meter range are observed in most wells, the assumption that these apertures are continuous in three dimensions produces hydraulic conductivity greater than that of those measured. Additional, more sophisticated well testing would be beneficial in assessing the validity of this conclusion. As a corollary, conduits with apertures in the centimeter to meter range might be contributing to flows in an undetermined fraction of the wells having no measured drawdown. Wells with very high transmissivity are known in the aquifer; for example, a 30-inch-diameter agricultural well near the downdip extent of freshwater flowed at 40 thousand gallons per minute and discharged to the Medina River (Rettman, 1991).

Numerical models require significant upscaling of permeability to match spring flows (Halihan and others, 2000; Scanlon and others, 2002; Lindgren, verbal communication, 2003). Upscaling can be accomplished either by distribution of high permeability through a wide zone (Klemt and others, 1979; Maclay and Land, 1988; Scanlon and others, 2002 or by addition of a smaller number of large aperture conduits (Lindgren and others, in preparation; Worthington, in preparation).

In the Barton Springs segment of the Edwards aquifer, detailed mapping of the potentiometric surface by collection of synoptic water levels in closely spaced wells has defined prominent, sharp to wide troughs (fig. 5a). A relict meter-scale phreatic conduit, now dry because of downward capture of flow, can be used to conceptualize the flow system. Note that a fragment of the former flow system is mapped as a cave, which has been truncated downstream by valley incision. A program of injection of dye tracers into recharge features and monitoring at wells and springs for the breakthrough of tracers has documented a complex of downward-converging, high-velocity conduit flow systems (fig. 5b).

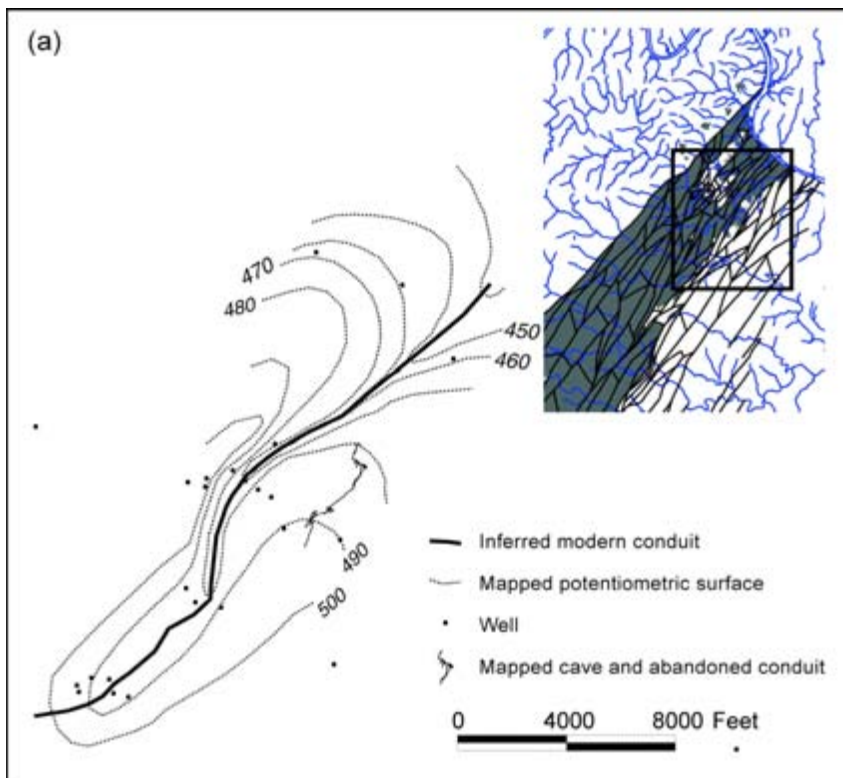
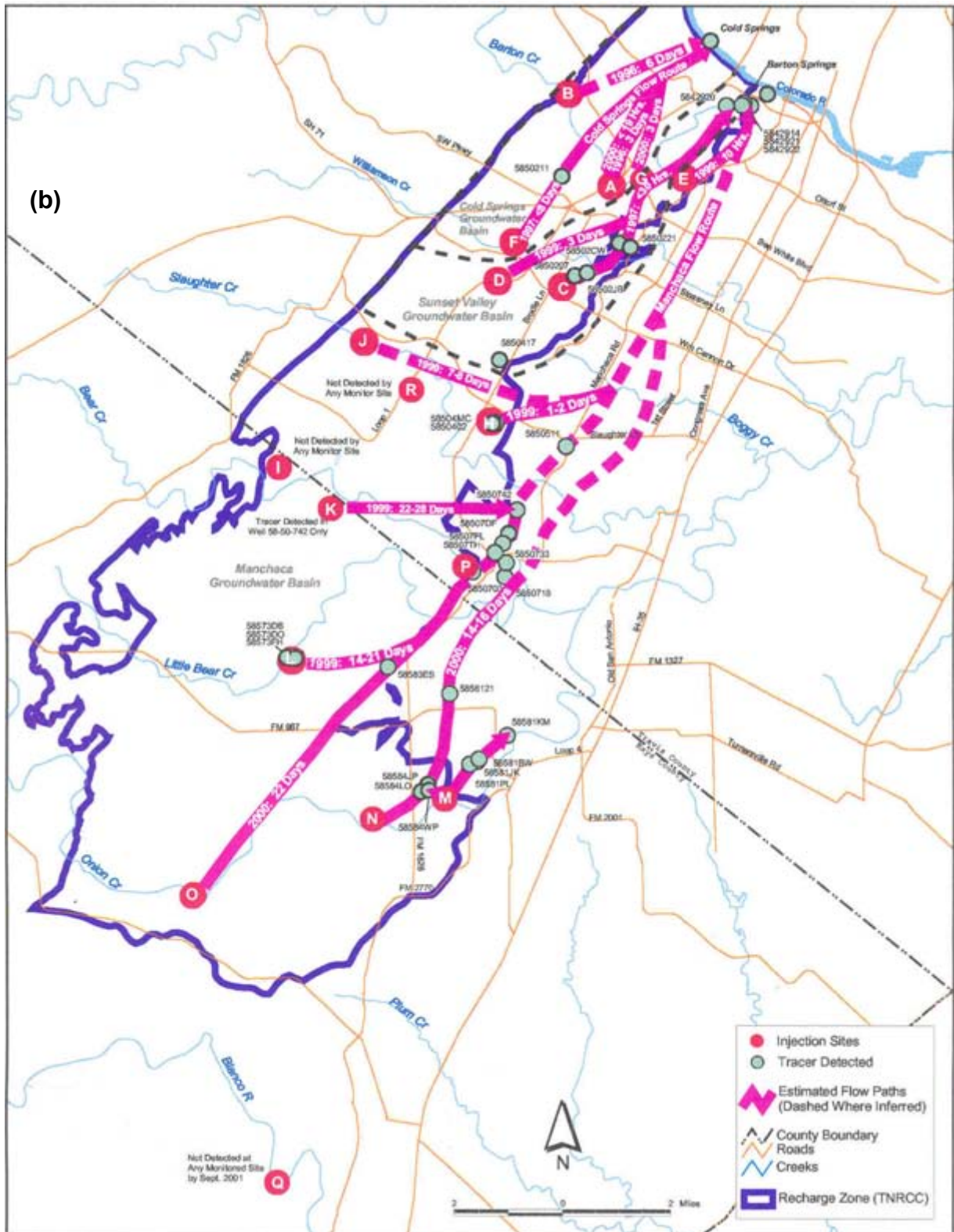


Figure 5. Information about conduit geometry from the Barton Springs Edwards aquifer. (5a) Trough in a detailed map of the Barton Springs aquifer (Hauwert and others, 2002), with superimposed detailed map of Airman's cave (Russell and others, 1974), a relict conduit that formerly supplied Barton Springs and provided a conceptual model for the aquifer characteristics that produced the trough. Cave and trough are strongly oriented parallel to faults mapped by Hauwert (digital communication, 2000) shown in detailed location map.



Tracer testing begun in the south-central Edwards aquifer has documented rapid breakthrough of tracer from wells to the nearby high flow springs (Ogden and others, 1986; Schindel, and others, 2002). Rapid transmission of contaminants from several spill sites (Mace and others, 1997; Schindel and others, 2002) also documents conduit flow systems active in the south-central segment of the Edwards aquifer.

In order to construct the numerical model for aquifer management now in preparation (Lindgren and others, in prep.), an estimate of the distribution of conduits was created by Worthington (in prep.). The data presented in this study are intended to validate the conceptualization of conduits presented in these two recent studies and further refine our understanding of conceptualization of flow. The overall results of this study, under way at the same the time as, and in communication with, the Lindgren and others and Worthington projects are in agreements about the presence and hydrologic significance of conduits. Many variations in interpretation of the geometry of conduits are noted; these areas will serve to focus future data collection.

Purpose of this study

The purpose of this study is to use existing data to characterize flow in the south-central (Balcones Fault Zone) segment of the Edwards aquifer, focusing on the contribution and interaction of fractures and solution-enlarged conduits. Indicators listed in the preceding review provide unequivocal evidence of the significance of conduits in the Edwards aquifer; however, detailed characterization of distribution, transmissivity, and storage of the conduit system is needed to model the flow system with high temporal resolution. This study uses low-cost available data to identify areas where conduits are inferred. The conclusions of this study will allow focused field work to more rapidly confirm the distribution of major conduits and measure critical aquifer properties.

METHODS

The methods used in this study were based on exploiting the large volume of existing data from the Edwards aquifer and exploring the utility of integrating multiple types of data. Data sets used include water levels, structural mapping, analyses of cave maps, water chemistry, and well hydrographs.

Water-level data

Recently the Edwards Aquifer Authority (Authority) led a consortium collecting water-level data during synoptic surveys, including more than 200 high-quality measurements collected during a short time period several times a year (digital communication, R. Esquilin, 2003). This data, in combination with other data sets, will lead directly to improvement in understanding the aquifer and model calibration. However, comparison of the density and distribution of the measurement points over the more than 40-mi² area of the aquifer with the data density that was used to define conduits in the Barton Spring segment (for example, fig. 5a) suggests that many troughs that are indicators of conduits may have been missed by this survey. In order to increase data density to prospect for additional conduits, we developed a method for incorporating

a large volume of historical water-level data archived by the TWDB into pseudosynoptic water-level maps. In order to explore the unconfined zone, we included water levels measured in the Trinity aquifer north of the Edwards.

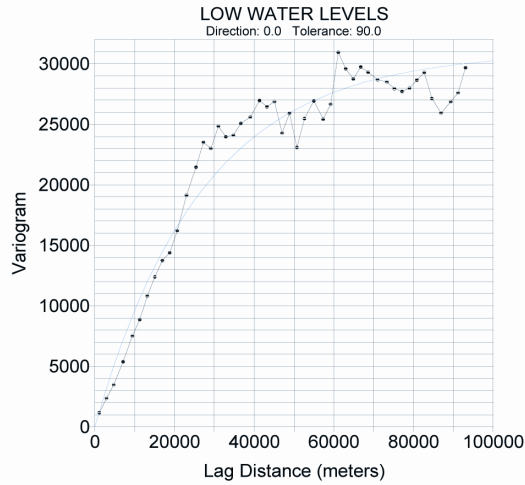
The greatest difficulty in using historical water levels is that the seasonal variation in water levels in many parts of the aquifer is greater than the variability resulting from transmissivity. We therefore developed a strategy for reducing this variability by assigning measurements to high, medium, and low stages. The hypothesis is that by reducing water-level variability by subsampling data by stage, variation in aquifer variability resulting from transmissivity (conduits) will be made more apparent. Conduit locations suggested by this method are then nominated for follow-up testing, which might include detailed synoptic water-level measurements, collection and analysis of well hydrographs and chemographs, and interception of natural or introduced groundwater traces.

Data were extracted from TWDB county well and water-level files for Kinney, Uvalde, Medina, Bexar, Comal, and Hays Counties and were formatted and merged into a single database containing well number, decimal latitude and longitude, aquifer code, depth to water (ft), land-surface datum (ft), and water level in feet from a sea-level datum. Several steps were used to remove major sources of error. We compared land elevation given in the well files with those extracted from 10- or 20-ft digital elevation models (DEM) downloaded from the Texas Natural Resources Information System (TNRIS) and deleted wells with greater than 10-ft deviation from the estimated ground level. Inspection shows that some well elevations are probably correct, but horizontal misslocation has created a mismatch between the real and mapped location elevations. We then screened the data for other anomalies and removed water levels lower than spring level and other outliers.

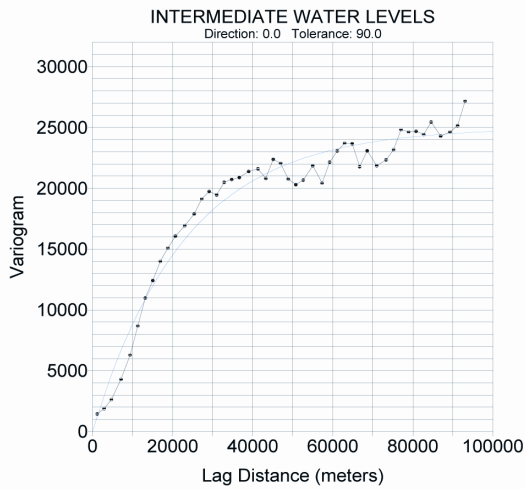
Pseudosynoptics were prepared by (1) inspection of monitoring-well records to define areas of generally similar water-level responses; (2) defining aquifer stages in these regions by preparing cumulative curves of water levels in index wells with long records of monthly water levels and dividing them to define the upper quartile of water levels, the intermediate two quartiles, and the lowest quartile; (3) dividing the time periods of record into high, medium, and low stages; (4) assigning historical water-level measurements, including index-well monthly averages, to a stage; (5) kriging the water levels for high, medium, and low stages using Surfer software; (6) removing obvious outliers; and then (7) repeating the kriging. Variograms developed during the kriging are presented in figure 6. Data were exported to ArcView as grid center points.

Data density was significantly increased over other data sets, with 681 wells in the low data set, 527 wells in the high set, and 914 wells in the intermediate set.

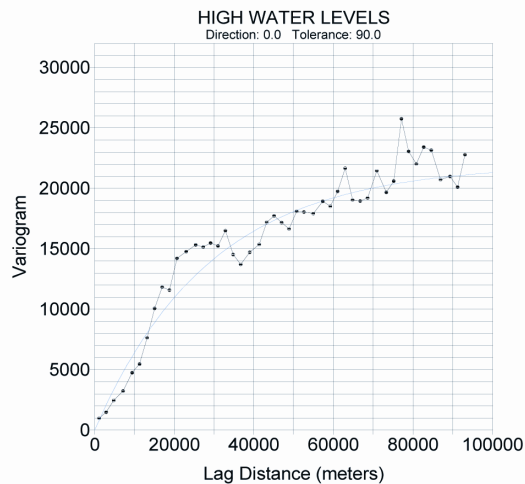
Variograms of Water Levels at High, Intermediate and Low Stages



Exponential Model
Scale = 22000
Length = 29000
Anisotropy: Ratio = 1, Angle = 0
Nugget Effect
Error Variance = 0
Micro Variance = 0



Exponential Model
Scale = 25000
Length = 23000
Anisotropy: Ratio = 1, Angle = 0
Nugget Effect
Error Variance = 0
Micro Variance = 0



Exponential Model
Scale = 31000
Length = 27000
Anisotropy: Ratio = 1, Angle = 0
Nugget Effect
Error Variance = 0
Micro Variance = 0

Figure 6. Variograms from kriged water levels.

Structural mapping and calculation of saturated thickness

In order to better assess the stratigraphic control on permeability, we refined structural interpretation in the recharge zone. Wells logged and entered in Authority files since our last study were photocopied, located, top Glen Rose contact picked by log correlation, and elevation (feet from sea-level datum) of this contact posted with other data. In addition, elevation of the mapped Glen Rose/Edwards contact was extracted from the DEM and used to control gridding. Elevation of the top Edwards contact was similarly refined as part of preparation of the numerical model. We compared the resulting structural interpretation with those made by other workers (Schulz, written communication, 2002; USGS digital data for Bexar, Comal, and Hays hydrostratigraphic member mapping). Errors identified during this comparison were corrected, although many variation interpretations remain unresolved. Contoured interpreted structure was gridded and a grid center elevation for the top of Glen Rose was exported to ArcView.

Saturated thickness within the Edwards for each stage was then calculated by subtracting water-level elevation from top Glen Rose elevation. Because Trinity wells are included in the mapping, water level is well controlled across the contact.

Analysis of cave maps

Caves provide significant but fragmentary information about the characteristics of conduits. Cave apertures fall at the high end of the range of centimeter to meter diameter conduits that dominate the Edwards flow system (Hovorka and Mace, 1997; Halihan and others, 2000). However, caves are generally entered and surveyed only under special circumstances that must be considered when interpreting data. Phreatic caves are entered when they have been abandoned and drained as a result of aquifer evolution. Long saturated sections of caves are rarely mapped because of prohibitive risk and logistics. In addition, caves can be mapped only where human-size connection to the surface has developed. It is common for previously unknown large caves to be found during trenching and drilling (fig. 4b). Relatively large (centimeter to decimeter aperture) openings typically continue beyond the mappable cave through zones of breakdown and sediment fill or into bedding-plane partings too small to allow human access, so that the cave represents only a fraction of the conduit. Most mapped caves are characterized by an overprinting of vadose modifications on features of phreatic origin. In order to use modeling cave geometry to infer conduit properties in the saturated zone it is necessary to recognize and subtract these overprints.

Many studies have focused on detailed analysis of cave systems as indicators of hydrologic evolution (for example, White and White, 1989; Palmer, 1991; Klimchouk and others, 2000). In this study, we decided to examine a large body of less detailed data to look for trends that can be used to infer the orientation of large-aperture conduits in the phreatic zone. Cave maps from the Edwards outcrop were photocopied from files of the Texas Speleological Survey (TSS) and from Veni (1988) and Elliott and Veni (1994). Maps that had adequate orientation and horizontal scale information were scanned, and TIFF images were created. A copy of the digital image files was donated to TSS archives to help them curate this data. Cave entrance locations were supplied by TSS and digital data by USGS (Clark, 2002). In order to protect caves, TSS classifies location data as propriety. In this report we have degraded the location data by using large dots on maps and truncating the location information in tables. We were successful in assembling all required components: a map with a north arrow, a horizontal scale, and an entrance location for 129 caves.

Cave map patterns were classified as (1) linear, (2) oblate, or (3) vertical. We then imported the cave map images into an image analysis program (ScionImage Beta Release 4), oriented and scaled them, and measured the direction of maximum elongation, which was recorded in the data table. We then plotted the location of cave entrances on GIS and extracted other orientations that we hypothesized might control cave elongation. These are (1) orientation of dominant faults bounding the block in which the cave is located and (2) inferred local modern hydrologic gradient. Faults were estimated from the revised structure map of the recharge zone. We did not have data to define the modern local hydrologic gradient in detail near any of the caves. Therefore, we tested hypotheses that the aquifer is so permeable that flow would occur down a local gradient toward the nearest discharge point, and that caves might be preferentially elongated in this direction. This possible local gradient was then estimated from the cave mouth to the nearest discharge point in a valley as defined by the 7.5-minute DEM. We then classified the caves according to which cave orientations matched the map orientations (regional structural trend or possible local gradient) within $\pm 10^\circ$.

Water chemistry

Water chemistry for the Edwards and Trinity aquifers was extracted from TWDB county water-quality tables and merged with county well files for Kinney, Uvalde, Medina, Bexar, Comal, and Hays Counties, which were then merged to create an overview of chemistry. This study was done to determine whether general chemical trends seemed useful in understanding conduit flow. More sophisticated analyses of mixing trends and rock-water interaction have been done for the Edwards (Land and Prezbindowski, 1981; Deike, 1990; Groshen and Buszka, 1997), especially focusing on downdip saline water. This type of analysis was not attempted within the scope of this study.

We used online geochemical data from Comal, Bexar, Medina, Uvalde, and Kinney Counties compiled and curated by the TWDB in order to calculate and rank the extent to which dilute water was approaching calcite or gypsum saturation. Because the data are compiled from various sources, TWDB provides a reliability estimate with its data. A check of hardness and alkalinity values shows that they are consistent with its

definition (assuming that properties were determined by titration while ions were determined by atomic sorption). Because calcite saturation index (*SI*) is very sensitive to pH and HCO_3^- activity, we want to consider only charge-balanced analyses. Samples with large charge unbalance were eliminated. Two series of runs were performed on geochemical speciation code PHREEQC2.8 (see Appendix I for input files): (1) data used as such, including charge imbalance if any, and (2) pH computed by the code so that the solution was charge balanced. In both cases, the system was assumed closed (no gas exchange). An analysis was ranked as acceptable when the difference in *SI* for calcite between types of run was less than 0.2. This resulted in 1,171 analyses retained out of a total of 6,056. When temperature data were missing, global average temperature (26.1) was used instead. Temperature does not have a large impact on results. Our approach is focused on geographic distribution, which complements more traditional geochemical analyses such as Groschen and Buszka (1997).

Well hydrograph separation

Groundwater flow in karst can be divided into several components: namely, diffuse or matrix flow (baseflow), flow through fractures, and flow through large conduits (quickflow). Typical analyses of flow-parameter collection systems (pump tests, numerical model calibration) generate only an integrated picture of those components. The goal of this analysis was to show that it is possible to discriminate among flow components and to extract information that could be used in dual permeability numerical modeling. High-sampling-rate well hydrographs are particularly well suited for that task. This approach has several advantages over pump tests. There is no water to dispose of, the aquifer is tested in natural conditions, and each storm is a different test. We screened USGS monthly well records to identify significant recharge events that could be analyzed for recession. We then requested 15-minute water-level records for selected events. High-frequency records for saline transect wells were made available by San Antonio Water System, and records from wells in the recharge zone were made available by the Edwards Aquifer Authority.

Response to pressure pulses (precipitation then recharge, atmospheric pressure variations) is a function of aquifer hydraulic diffusivity. Hydraulic diffusivity is defined as the ratio of transmissivity to storage coefficient (specific yield if unconfined) or equivalently of hydraulic conductivity to specific storage. When recharge water abruptly enters an aquifer, it creates a pressure wave that propagates through the subsurface, creating a surge in water levels in wells and in spring discharge. The same way slug tests characterize an aquifer volume smaller than that of a pump test, diffusivity values over varying volumes can be obtained according to the relative locations of the input signal and receptor. Best data are provided by intense storms of short duration followed by little rain during the recovery period. In addition to information provided by the lag and attenuation of the signal, an analysis of transient recovery of the water level in a well (also called recession curve by analogy to stream flow) after the passage of the pressure pulse can differentiate between different types of flow (matrix, fracture, or conduit). As in stream flow, well hydrograph recession curve often appears to follow an exponential decay model ($Q = \exp(-\lambda t)$) and can be approximated as a straight line on a semilogarithmic scale as expressed in Equation 1.

$$\ln Q_2 / Q_1 = -\lambda(t_2 - t_1) \quad (1)$$

where Q_1 and Q_2 are flow rates at times t_1 and t_2 . The parameter λ is the slope of the straight line approximating the recession curve in the semilog space. Stream-flow recession curves often show multiple slopes. Slope variations are generally attributed to stream-channel storage, bank and soil storage, and groundwater storage that successively reach a stream gauge. The rising limb is mainly a function of the precipitation event, whereas the recession limb is effectively independent of the nature of the rain event. A method of recession curve analysis for well hydrographs was devised by Shevenell (1996) that relies only on water level and not on discharge. The method generates ratios of flow between the different flow components, as well as ratios of the storativity, and, under some assumptions, the flow components themselves as well.

Details of the method are presented in Shevenell (1966) and Powers and Shevenell (1999). Water levels Y_1 and Y_2 at times t_1 and t_2 of the well hydrograph recession curve can be expressed by:

$$\ln(Y_1/Y_2)/(t_2 - t_1) = \lambda = \ln(Q_1/Q_2)/(t_2 - t_1) \quad (2)$$

Assuming a simple recession curve for the sake of equation derivation, the available volume in storage at time t is the area under the curve between time t and large times:

$$V_t = \int_t^{\infty} Q dt \quad (3)$$

$$V_t = \int_t^{\infty} Q dt = \int_t^{\infty} \exp(-\lambda t) dt = \left[-\frac{1}{\lambda} \exp(-\lambda t) \right]_t^{\infty} = \exp(-\lambda t) / \lambda \quad (4)$$

$$V_t = Q_t / \lambda \quad (5)$$

where V_t is water storage producing flow rate Q_t . The volume of water in storage at any time is:

$$V_t = ASY_t \quad (6)$$

where A is drainage area, S is specific yield or storativity, and Y_t is water level at time t . Equating Equations 5 and 6 yields:

$$ASY_t = Q_t / \lambda \quad (7)$$

The previous derivation is also valid in the case of multiple-slope recession curve when applied within a time range with a constant slope. The first slope, typically the steepest, encompasses all flow regimes but is dominated by conduit flow. The last slope, typically the most flat, is characteristic of matrix or diffuse flow.

If the assumption of a constant drainage area A for the different flow types is made, the ratio of different S parameters can be calculated. If the assumption of a constant drainage area A is invalid, the ratio of drainage areas must be provided. Direct pipe flow between a sinkhole and conduits is one of these cases.

The analysis can go farther, given the following simplifying assumption on hydraulic diffusivity. Hydraulic diffusivity of the system can be calculated from Rorabaugh (1964). Baseflow recession q without recharge in a parallel-sided darcian aquifer is given by:

$$q = 2T \frac{h_0}{L} \exp\left(-\frac{\pi^2 T t}{4L^2 S}\right) \quad (8)$$

where T is transmissivity, h_0 is initial head at start of regression, L is distance from groundwater divide, S is storativity, and t is time. For two flow rates Q_1 and Q_2 at times t_1 and t_2 , Equation 8 can be written:

$$\ln(Q_1 / Q_2) = \frac{\pi^2 T}{4 S} (t_2 - t_1) \frac{1}{L^2} \quad (9)$$

Combining Equations 2 and 9 yields:

$$\lambda = \frac{\pi^2 T}{4 S} \frac{1}{L^2} \quad (10)$$

Knowledge of either geometry of the drainage area or hydraulic diffusivity will allow calculation of the other.

RESULTS

Water-level mapping

All three pseudosynoptic water-level (figs. 7, 8, 9) maps show two main trends: (1) a steep and fairly uniform gradient of more than 100 ft/mi between Edwards and Trinity aquifers and (2) a gradual gradient from east to west ranging from 1.2 ft /mi in the east part of the aquifer steepening to 2.8 ft/mi in eastern Medina County. Overprinted on these regional trends are a number of troughs and divides. Prominent in all three pseudosynoptic maps is a wide trough that extends westwards from central Bexar County to western Medina County (marker A-B in figs. 7, 8, 9). This trough is clearly defined in the synoptic surveys compiled by EAA (fig. 10) and has been recognized as a zone of high transmissivity in previous models (Klemt and others, 1979; Maclay and Land, 1988; Painter and others, 2002).

In all three pseudosynoptic water-level maps, the trough can be traced westward to Uvalde County (figs. 7, 8, 9 “D”). West into Kinney County the trough becomes broad and poorly defined (figs. 7, 8, 9 “C”).

Worthington (in prep.) conceptualized a dendritic pattern of conduit connection from the recharge zone to the confined zone. Numerous subtle troughs or notches in the steep gradient between Glen Rose and Edwards aquifers suggest locations of more transmissive zones (or example E and G on figs. 7, 8, 9). Data density is inadequate to define sharp troughs or subtle complexity of flow across the high-throw faults that separate the Glen Rose from the Edwards Formation.

High porosity and permeability in deepest parts of the aquifer near the fresh-saline interface suggest that flow may be focused in this area. A half trough (gradient toward the interface) is recognized along most of its extent from the springs to eastern Medina County (G on figs. 7, 8, 9). West of “G,” data are inadequate to define the gradient in the deepest part of the aquifer.

Subtracting the high pseudosynoptic from the low pseudosynoptic yields a map (fig. 11) of water-level variability in the unconfined aquifer and pressure in the confined aquifer. Highest changes in water levels are in western Medina County and eastward along the A-B trough. An area in southern Hays County has poor data density because it lacks an index well for stages to be assigned correctly to water levels. Areas where water levels are higher in the low stage than in the high stage occur in the Trinity aquifer, toward the edge of the data and where data are sparse. This error is likely a mixture of Trinity wells that do not respond harmoniously with Edwards wells and gridding edge effects.

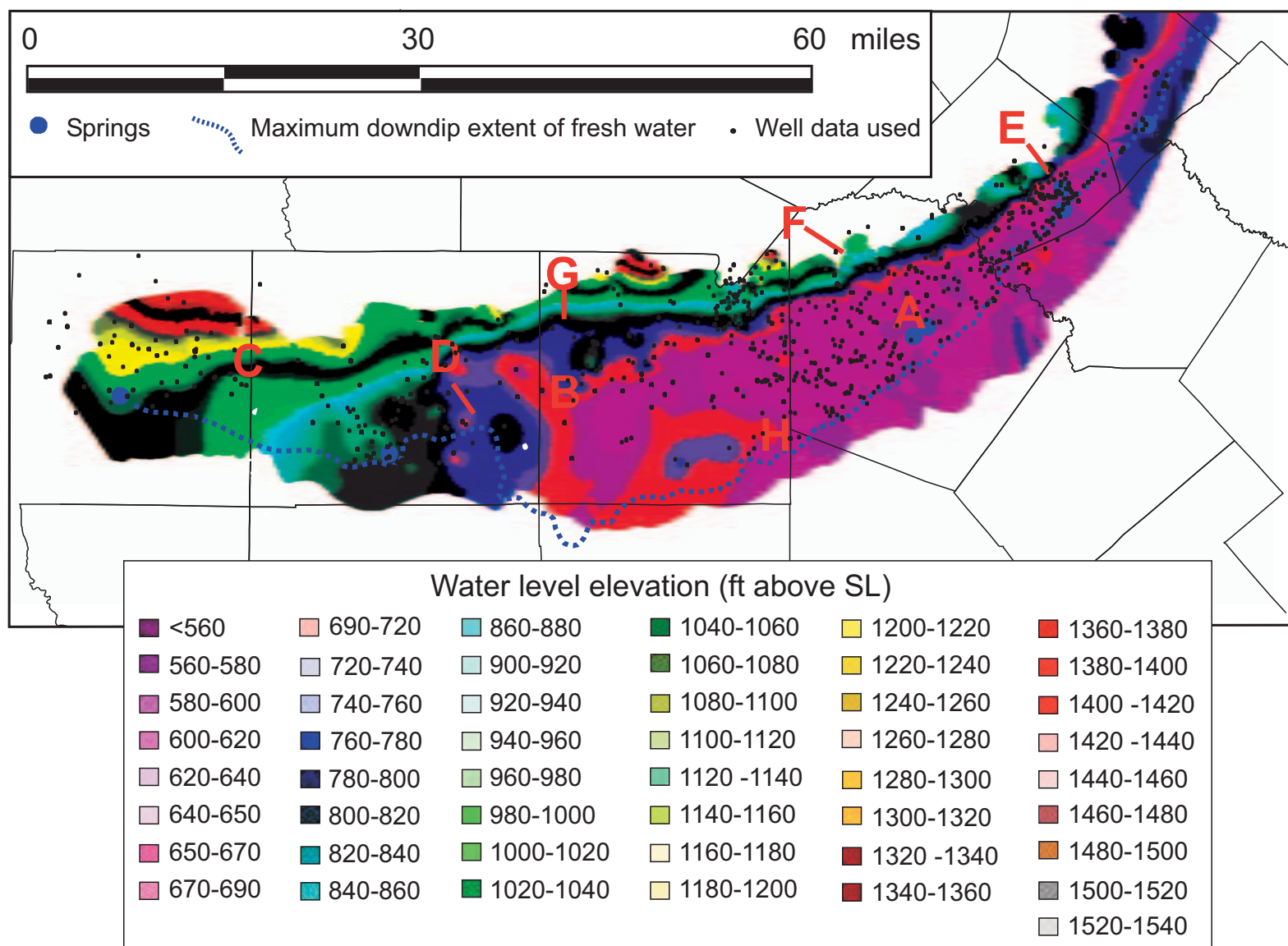


Figure 7. Low-stage pseudosynoptic. Historical water levels from time periods corresponding to lowest quartile of water levels in index wells are kriged and gridded. Letters are keyed to features discussed in the text.

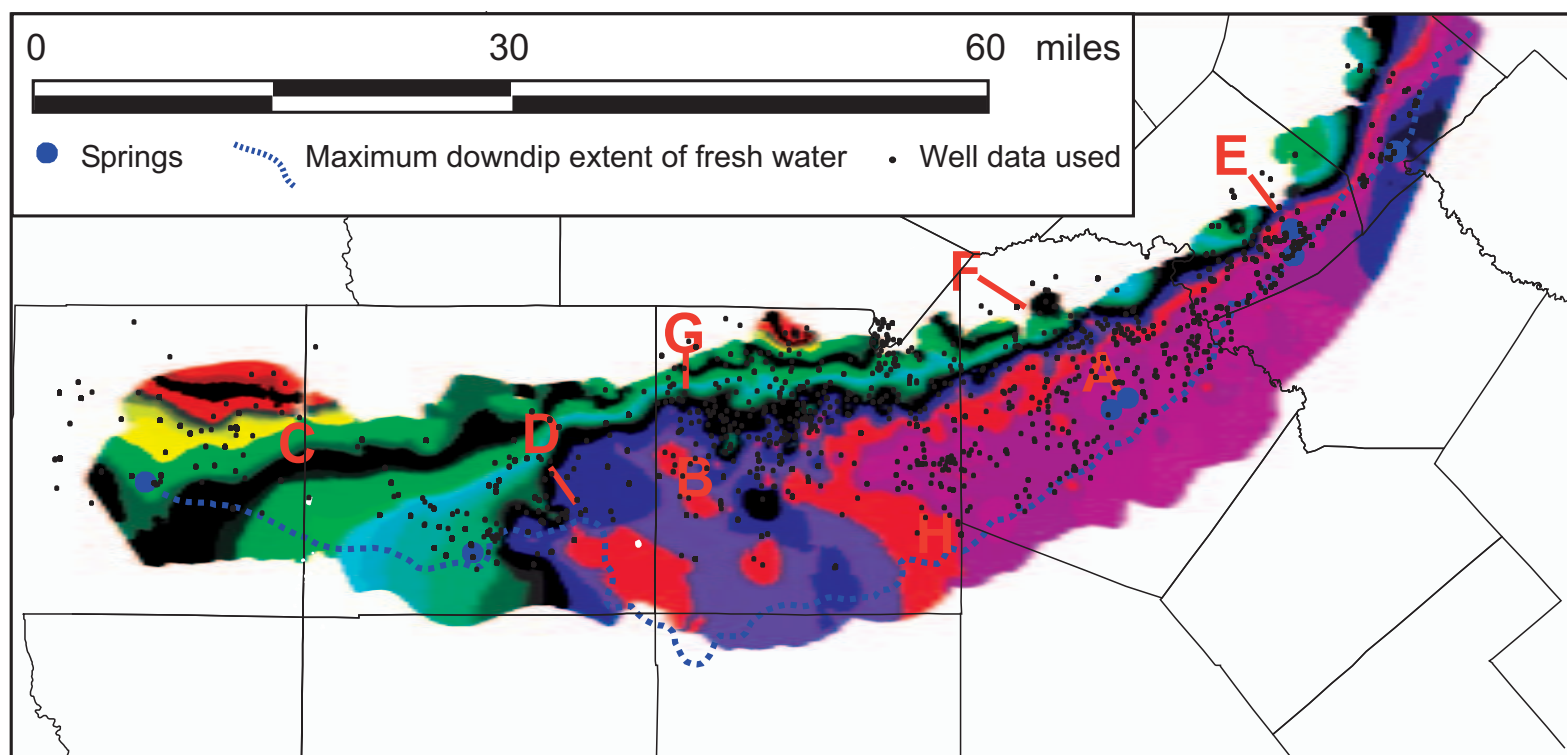


Figure 8. Intermediate-stage pseudosynoptic. Historical water levels from time periods corresponding to middle two quartiles of water levels in index wells are kriged and gridded. Letters are keyed to features discussed in the text. Color scale same as that for figure 7.

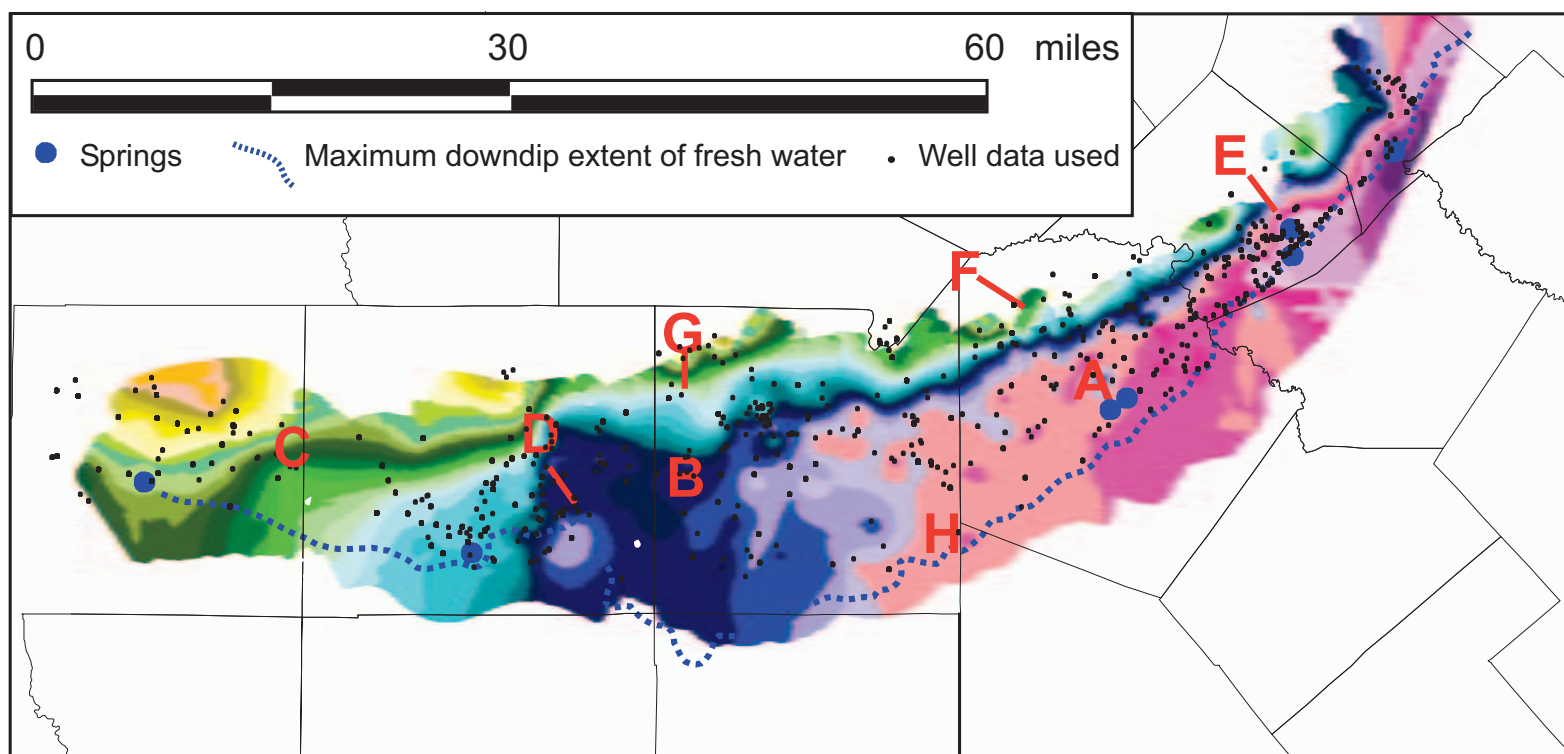


Figure 9. High-stage pseudosynoptic. Historical water levels from time periods corresponding to lowest quartile of water levels in index wells are kriged and gridded. Letters are keyed to features discussed in the text. Color scale same as that for figure 7.

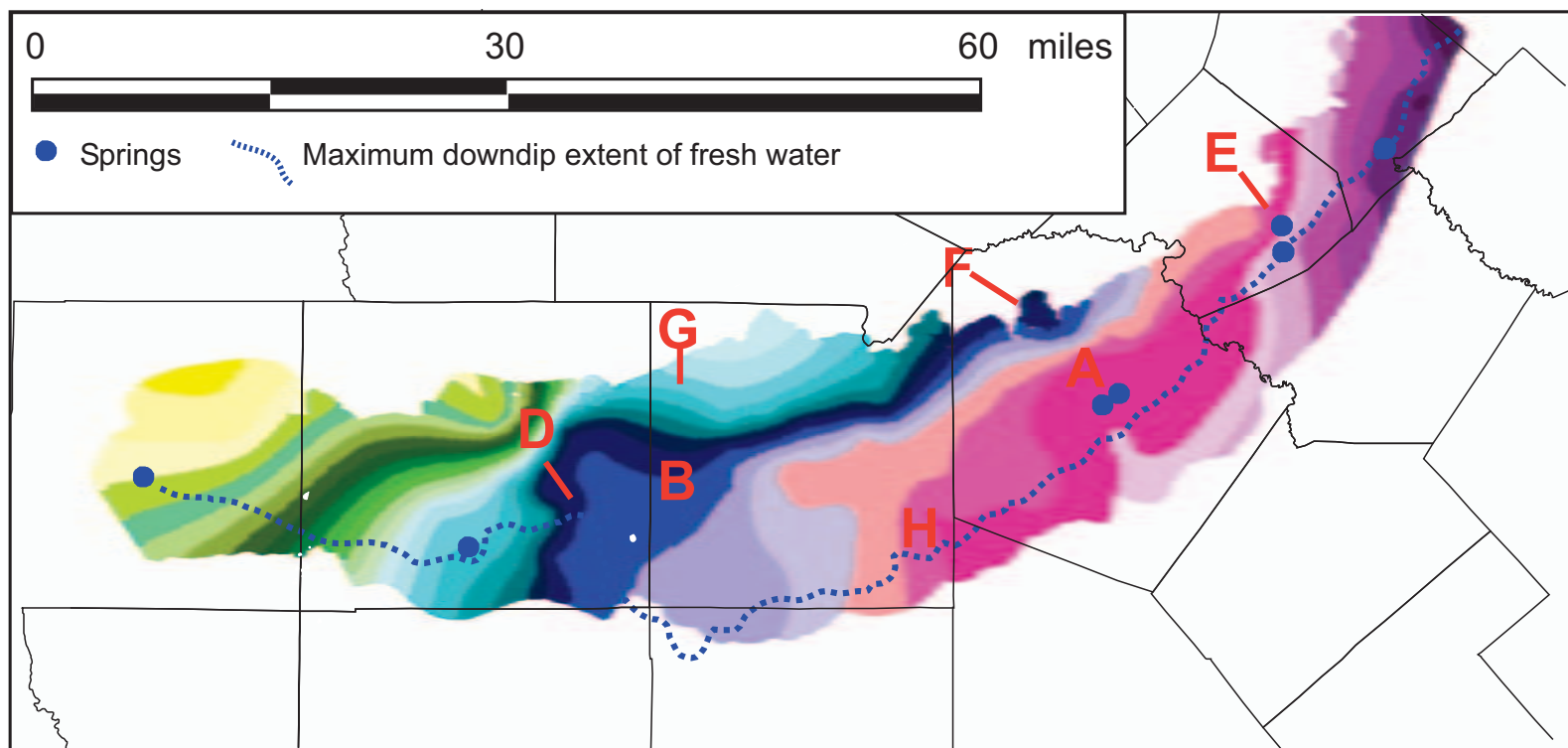


Figure 10. Gridded provisional synoptic data from October 1999 (R. Esquilin, EAA digital data, 2003), showing the well-defined trough (compare with figure 7 A-B).

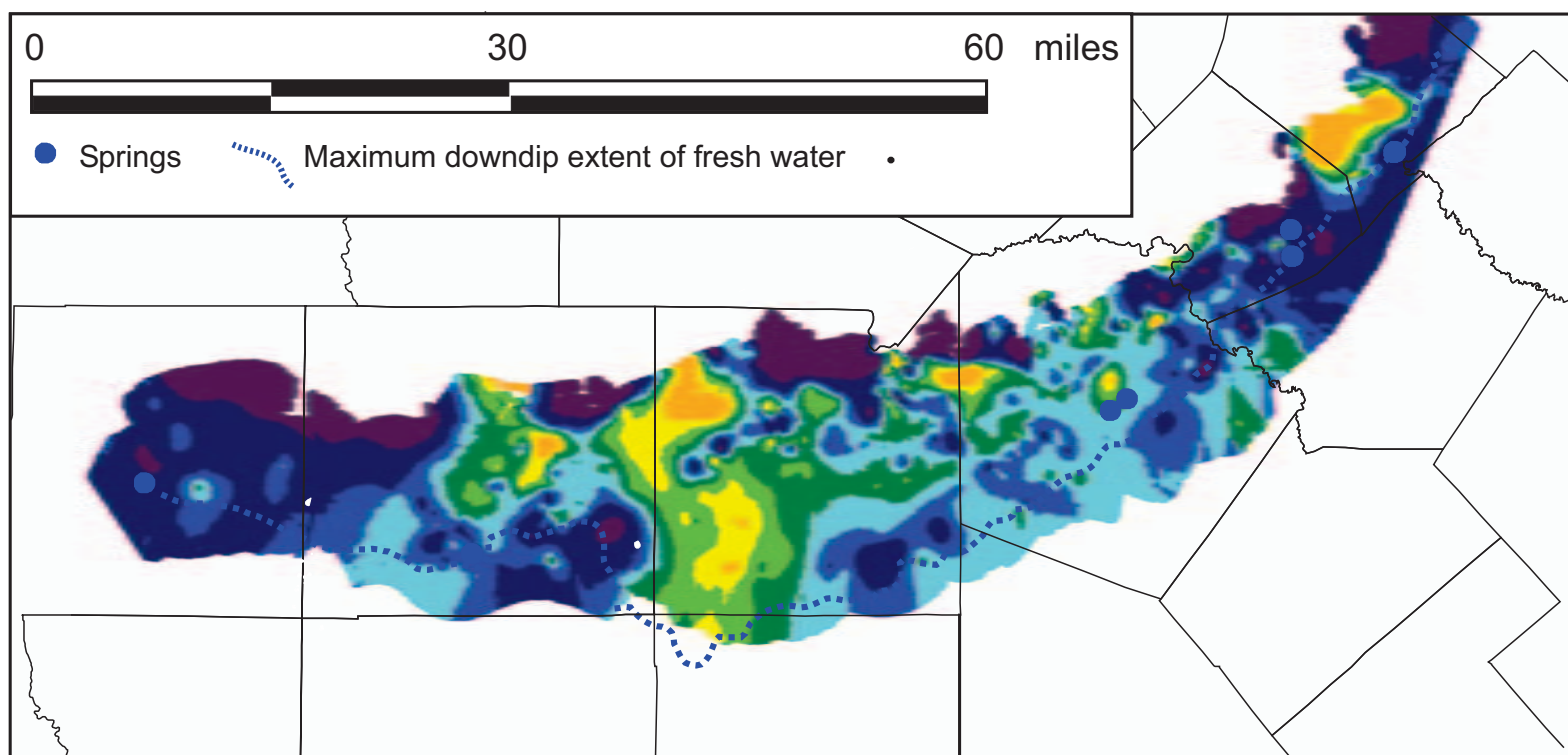


Figure 11. Water-level change shown by subtracting low from high pseudosynoptic. Color scale same as that for figure 7.

Intersection of structure and water level

Rock properties interact with flow systems so that karst conduits develop differently in different stratigraphic intervals. To begin assessing these relationships, we calculated thickness of the Edwards that is saturated (water-level elevation—top Glen Rose elevation). Saturated thickness was classified into five categories. Thickness less than zero indicated that the Edwards is unsaturated and the top of groundwater is within the Glen Rose Formation. Thicknesses of 1 to 250 ft were saturated mostly in the Kainer Formation or stratigraphically equivalent lower part of the Devils River or West Nueces-McKnight Formations in the west. At a saturated thickness of 250 to 500 ft, the top of groundwater is in the Person Formation, upper Devils River, and Salmon Peak. The Edwards Group thickens toward the west (fig. 1), so a transition zone from 500 to 600 ft is mapped. In the confined zone, the Edwards is fully saturated, with saturated thickness greater than 600 ft. Minimum saturated thickness is found during low stage (fig. 12a).

Comparison of saturated thickness with that of the Edwards outcrop (fig. 12b) shows that in Comal, Hays, Bexar, and Medina Counties, the Edwards Formation beneath the Kainer and lower Devils River outcrop is unsaturated, and saturated Person is found only where post-Edwards units (Del Rio, Buda, and younger units) crop out. The Edwards Group is only partly saturated in significant parts beneath the post-Edwards units (Del Rio, Buda) in western Bexar and eastern Uvalde Counties, and in grabens in Comal County.

In the west part of the area, corresponding to Maverick Basin facies (fig. 1), up to 250 ft of section is saturated in the lower Edwards Group (West Nueces and McKnight Formations) outcrop. Up to 500 ft of section is saturated beneath the Salmon Peak Formation outcrop. As the section becomes thicker to the south, it is incompletely saturated almost to the fresh-saline interface.

We calculated the saturated thickness at intermediate and high-stage pseudosynoptics; however, the patterns were similar because the dip is steep relative to somewhat suppressed changes in water level near outcrop.

Cave map analysis

Edwards caves are mostly small and have rather simply mapped geometries. We inventoried the distance from the cave entrance to the maximum extent of mapped cave for 236 caves photocopied from the TSS archives and determined that 90% of mapped Edwards cave footprints lie within a 250-ft circle centered on the opening (fig. 13). However, the longest Edwards cave inventoried is more than 3,000 ft long.

We identified only 129 Edwards caves that had data complete enough for the proposed analyses, and these were clustered in Bexar, Hays, and Travis Counties (fig. 14), limiting the potential for analysis of variation across the aquifer. Of these, 44% of caves could not contribute information toward our understanding of the phreatic flow system because they are either dominantly vertical caves formed by vadose processes or they are weakly elongated phreatic caves. Of the remaining caves, structural controls proved to be the main contributor of morphologies of caves in this

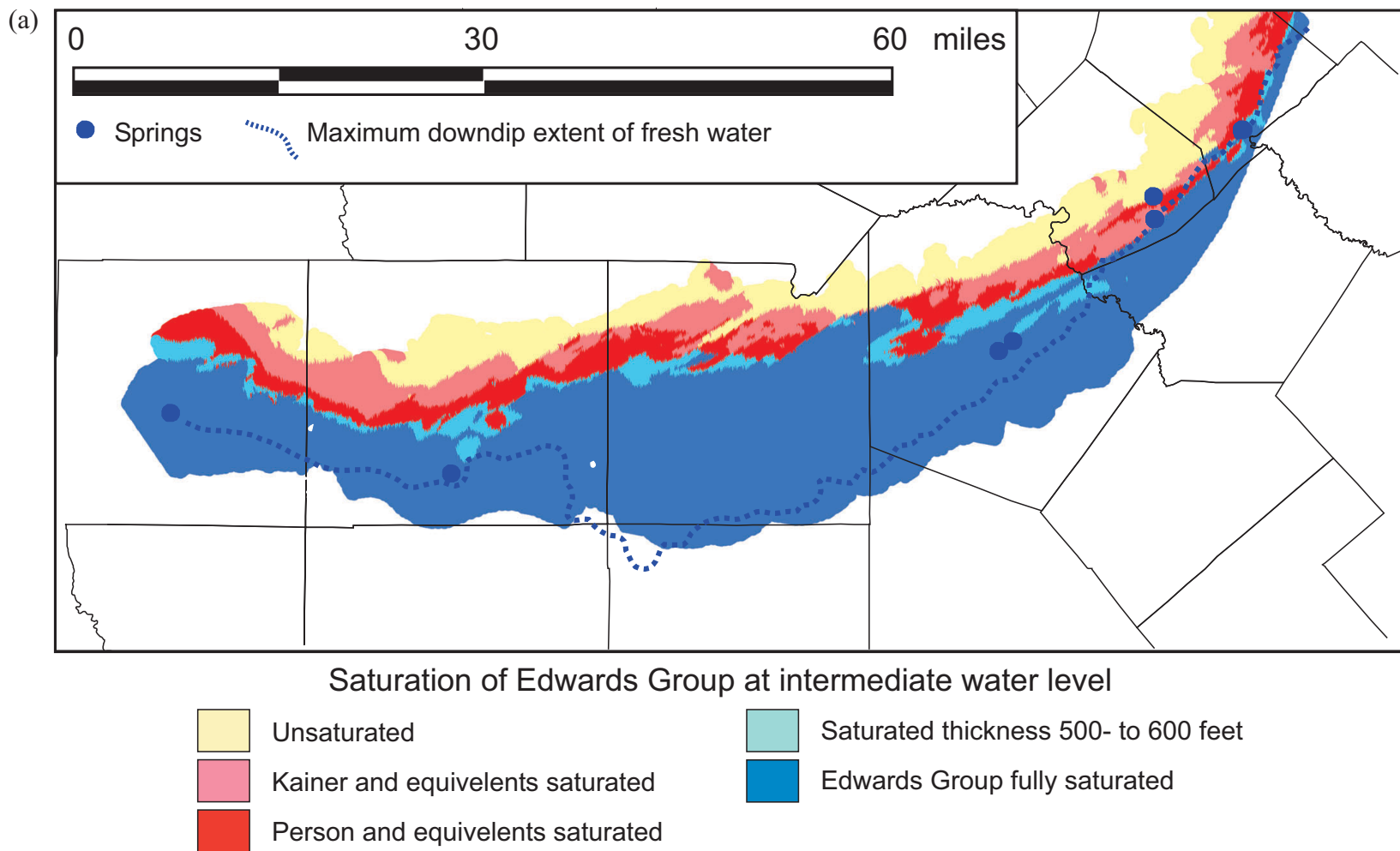
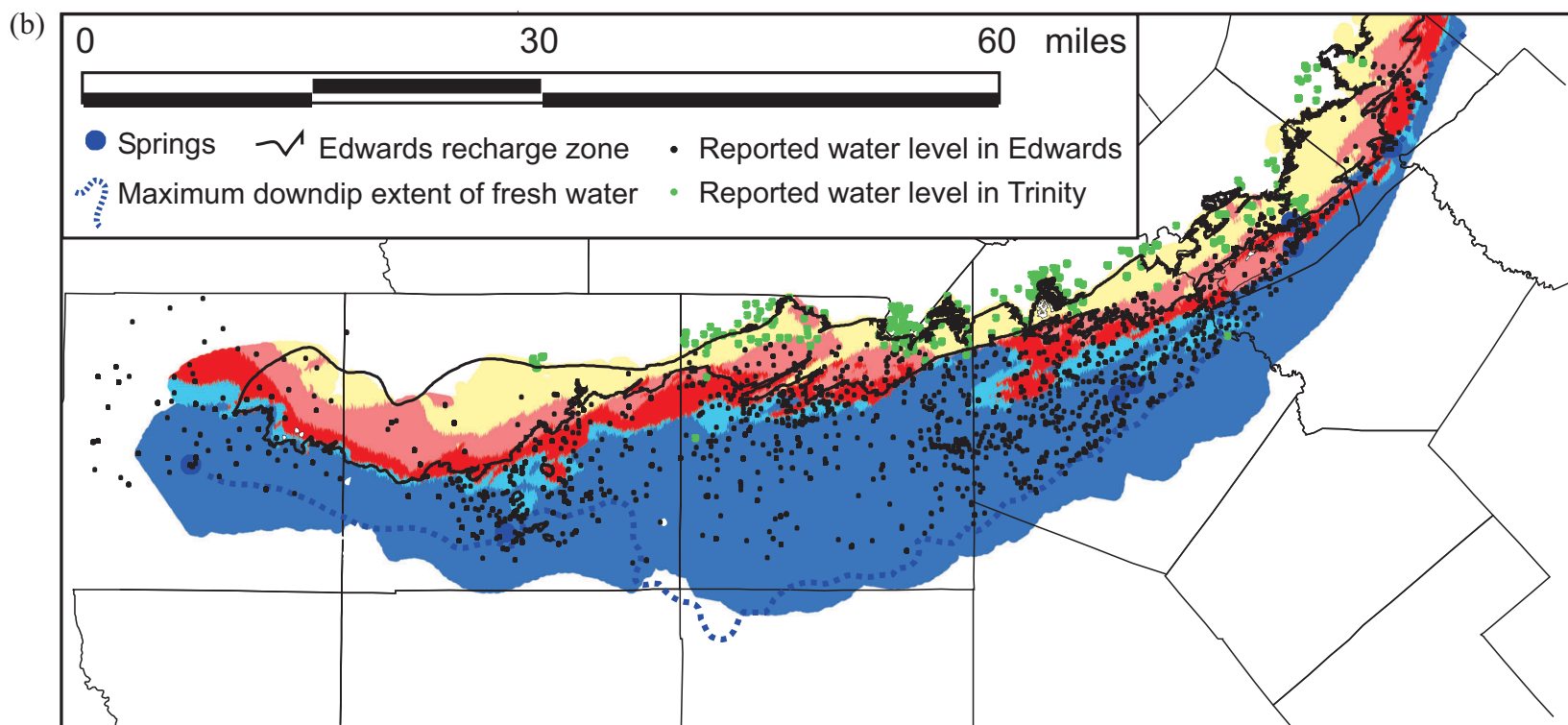


Figure 12. Saturated thickness of the Edwards Formation. (a) Saturated thickness map.



Saturation of Edwards Group at intermediate water level

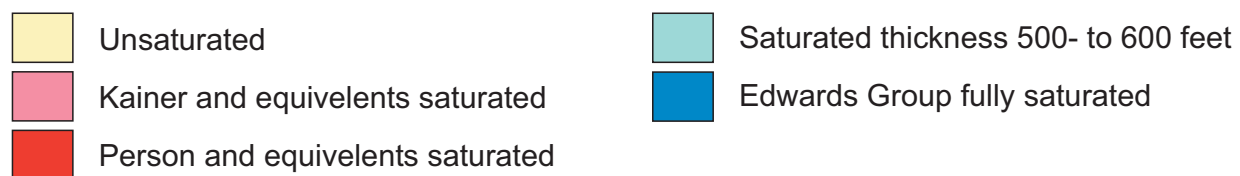


Figure 12. Saturated thickness of the Edwards Formation. (b) saturated thickness overlain by the outcrop pattern and reported producing aquifer from TWDB records.

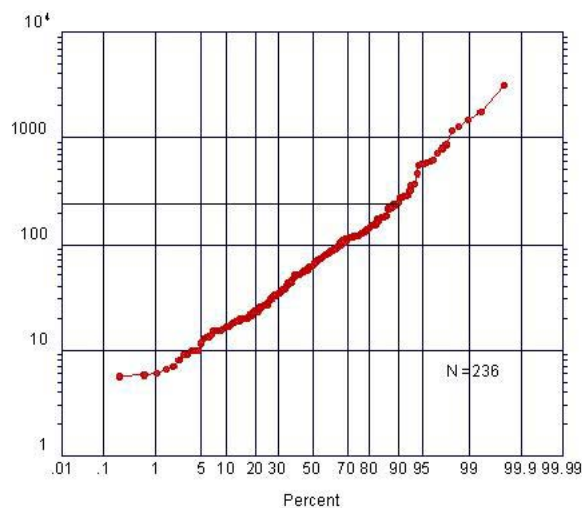


Figure 13. Cumulative frequency of the maximum distance in map view of the edge of the mapped cave “footprint” from the entrance. Note that this analysis is truncated by the pragmatic definition of a cave as a space that can be entered by humans and by lack of interest in mapping very small caves.

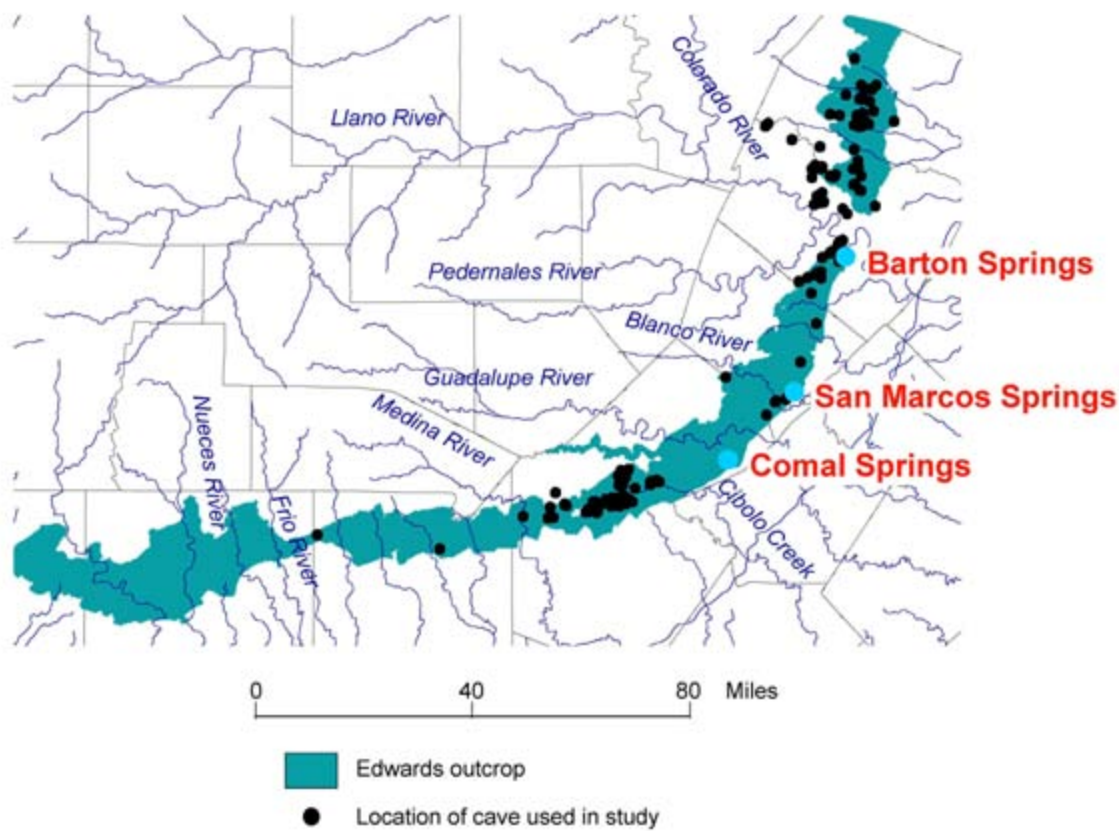


Figure 14. Distribution of caves analyzed. High-quality cave maps with entrance location information were clustered geographically possibly because of accessibility to cavers.

region, with 31% of 129 caves studied showing strong elongation parallel to mapped faults. Of these, 8% were also parallel to local gradient, as estimated from topography.

Only 5% were aligned parallel to local gradient and not regional structure. This amount is approximately the same as would be expected if the coincidence were random. The remaining 20% of caves were strongly elongated but not parallel to faults or gradient; these were inferred to be developed along local fracture trends. Dominant opening-mode fracture systems in an extensional tectonic setting (Ferrill and Morris, 2003) are expected to parallel major faults. Faults themselves may or may not be transmissive because of breccia, gouge, or cement. Other fracture trends are noted because of the complex geometry of the Balcones Fault Zone, relay ramps and folds, for example. Pre- and possibly post-Balcones fracture trends may also be expressed (Wermund and others, 1978).

Water quality

Karst processes are closely associated with surface and groundwater chemistry. In order to explore these relationships, we plotted a sample of water quality parameters on the same base used for exploration of conduits. We assume as a first approximation that salinity measured as total dissolved solids (TDS) is a proxy for residence time in the aquifer (fig. 15). The most saline waters would be found in the areas with the poorest connection, and the freshest water is found either in the recharge zone or in the fastest flow paths in or near conduits. The Glen Rose and the down-dip Edwards contain saline waters, with total dissolved solids (TDS) of down-dip water greater than 3000 ppm (fig 15a). Most Edwards waters are between 500 and 1000 ppm. A small number of the low salinity water samples were from deep in the aquifer. Glen Rose water salinity is more scattered, but about half the values are in the 1000 to more than 3000 ppm range, and the rest of the waters are similar to or fresher than the Edwards. A concept of fast flow paths bypassing more saline areas appears to be needed to account for the salinity distribution.

Gypsum dissolution is one of the principal contributors to salinity in the Edwards and Trinity aquifers. Gypsum is preserved within these units, and is actively undergoing dissolution. Highest saturations are noted within the Glen Rose Formation, but many water samples undersaturated (fig. 16), indicating that they bypassed gypsum-bearing units. Gypsum saturated or near saturation waters are also common in the saline parts of the Edwards. Gypsum saturation is low in the freshwater part of the Edwards, which has long been used as evidence that Glen Rose waters do not pervasively flow into the Edwards. However, the abundant low sulfate regions in the Glen Rose could contribute to the Edwards aquifer.

Calcite saturation provides a direct indicator of the role that water has had in karst processes. Only very fast moving water can remain undersaturated deep inside the aquifer. Surface and soil pore water is undersaturated with calcite because it has high HCO_3 as a result of interaction with atmospheric and soil gas CO_2 . Very undersaturated waters are found in Kinney County in the western part of the aquifer as well as an up-dip area of Comal County (fig. 17). However as water moves through pore spaces and small aperture fractures it will quickly dissolve calcite and approach saturation. Water that

recharges by turbulent flow through large diameter conduits can remain unsaturated. This is interpreted as the origin of very undersaturated water at depth in Medina, Bexar, Comal and Hays counties.

Nitrate (NO_3) is probably contributed to groundwater from surface sources, including agricultural and urban sources. Nitrate contamination is common in karst groundwater because recharge can occur with minimal storage in the root zone that would otherwise reduce nitrate content by plant uptake. High concentrations (greater than 30 ppm) of nitrate are noted at a number of locations in the Glen Rose outcrop, and a few locations near the Edwards recharge zone (fig. 18). A few isolated high concentration samples are noted in the deeper part of the Edwards aquifer. These samples are not diluted indicating that they have moved into the aquifer by fairly direct flowpaths, either down poorly completed wells or through conduits.

(a)

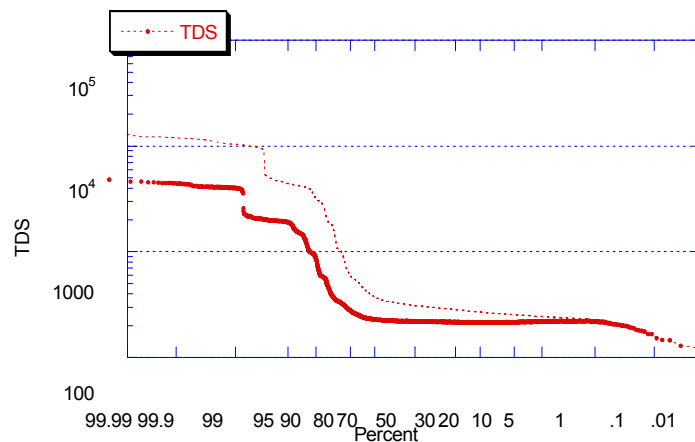


Figure 15. TDS in ppm from the TWDB water quality database. (a) Cumulative frequency plot.

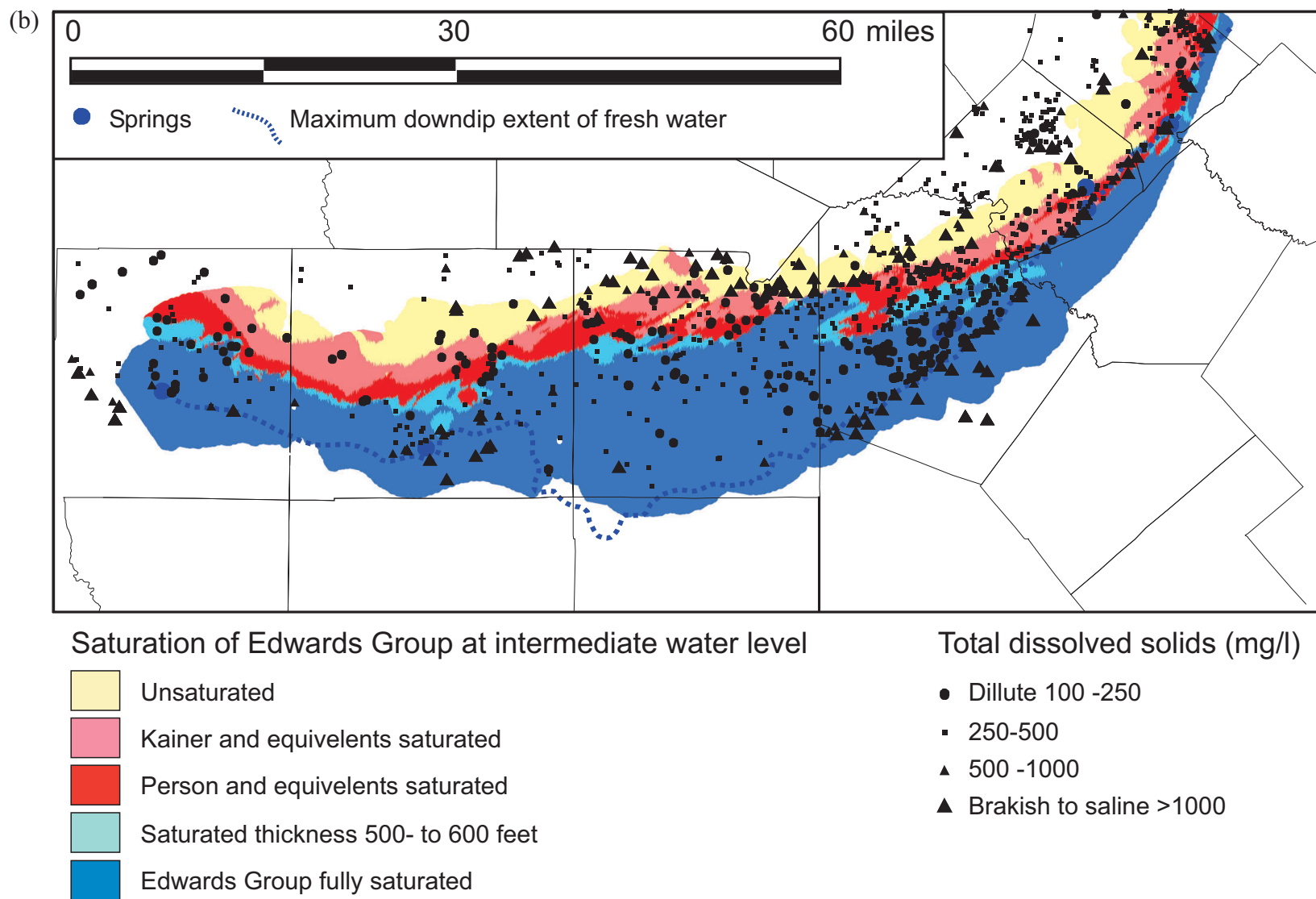


Figure 15. TDS in ppm from the TWDB water quality database. (b) map distribution plotted on the saturated thickness base (low pseudosynoptic).

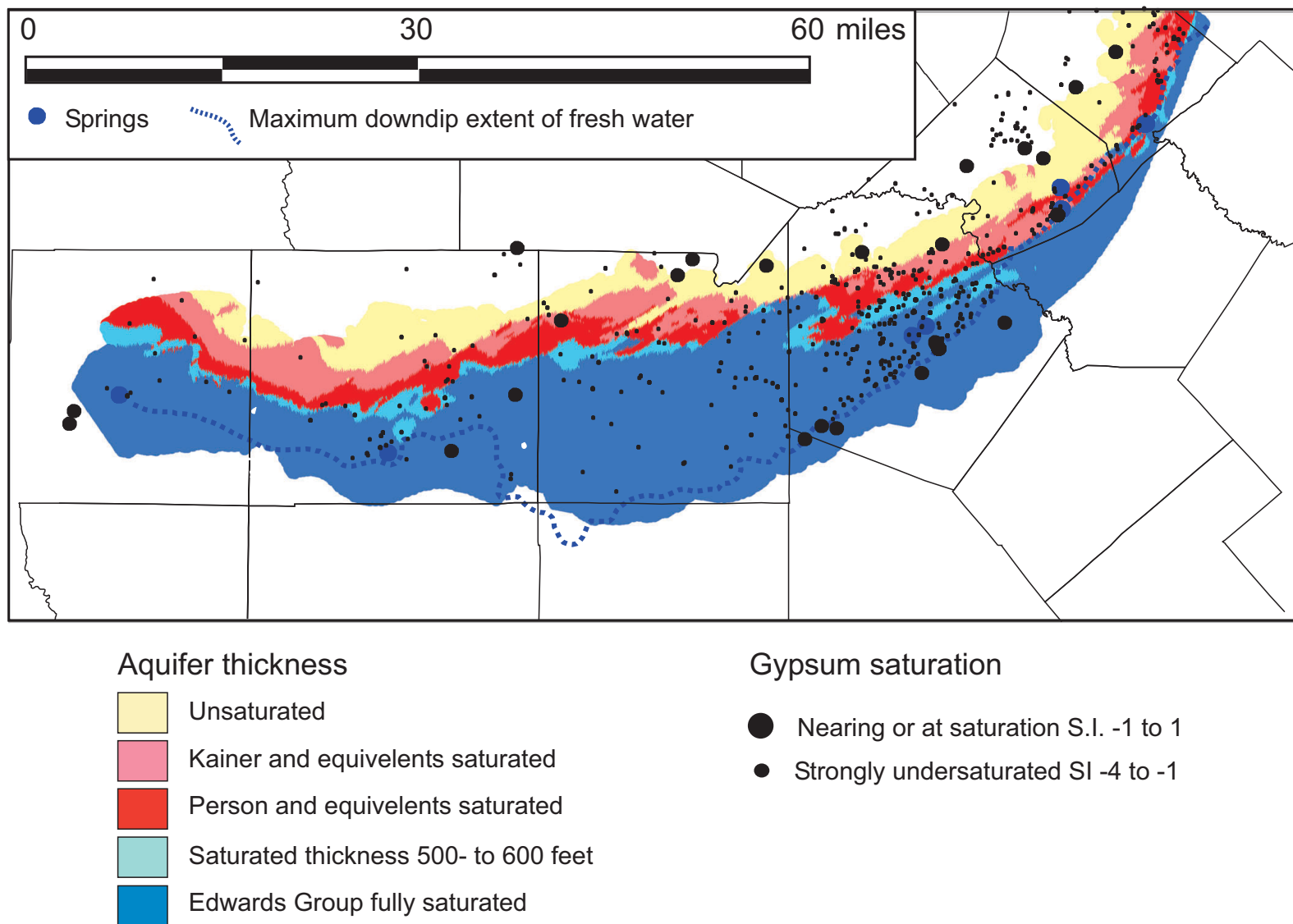


Figure 16. Relative gypsum saturation, from “saturated near 1” to “undersaturation (strongly negative numbers)” plotted on the saturated-thickness base (low-pseudosynoptic water-level map).

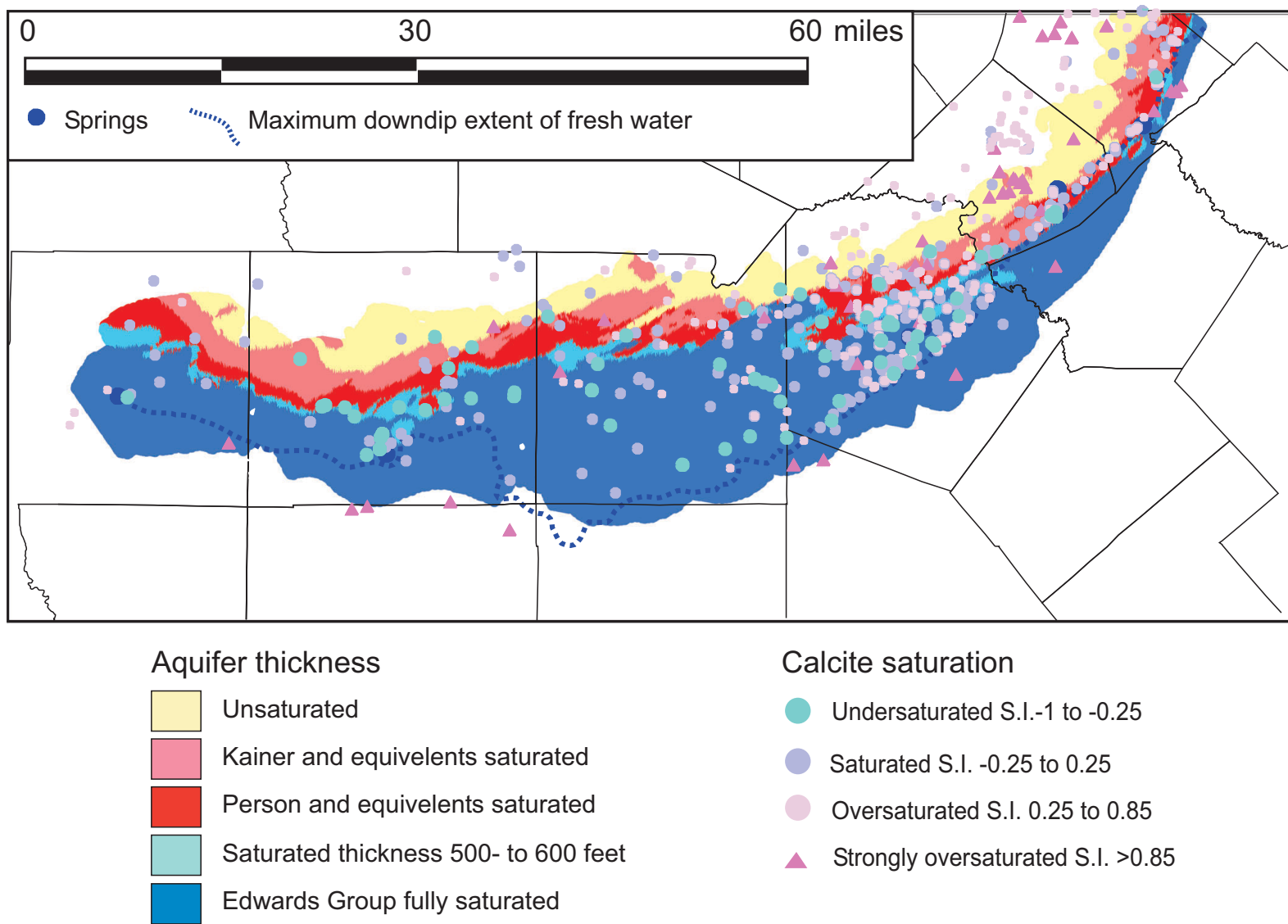
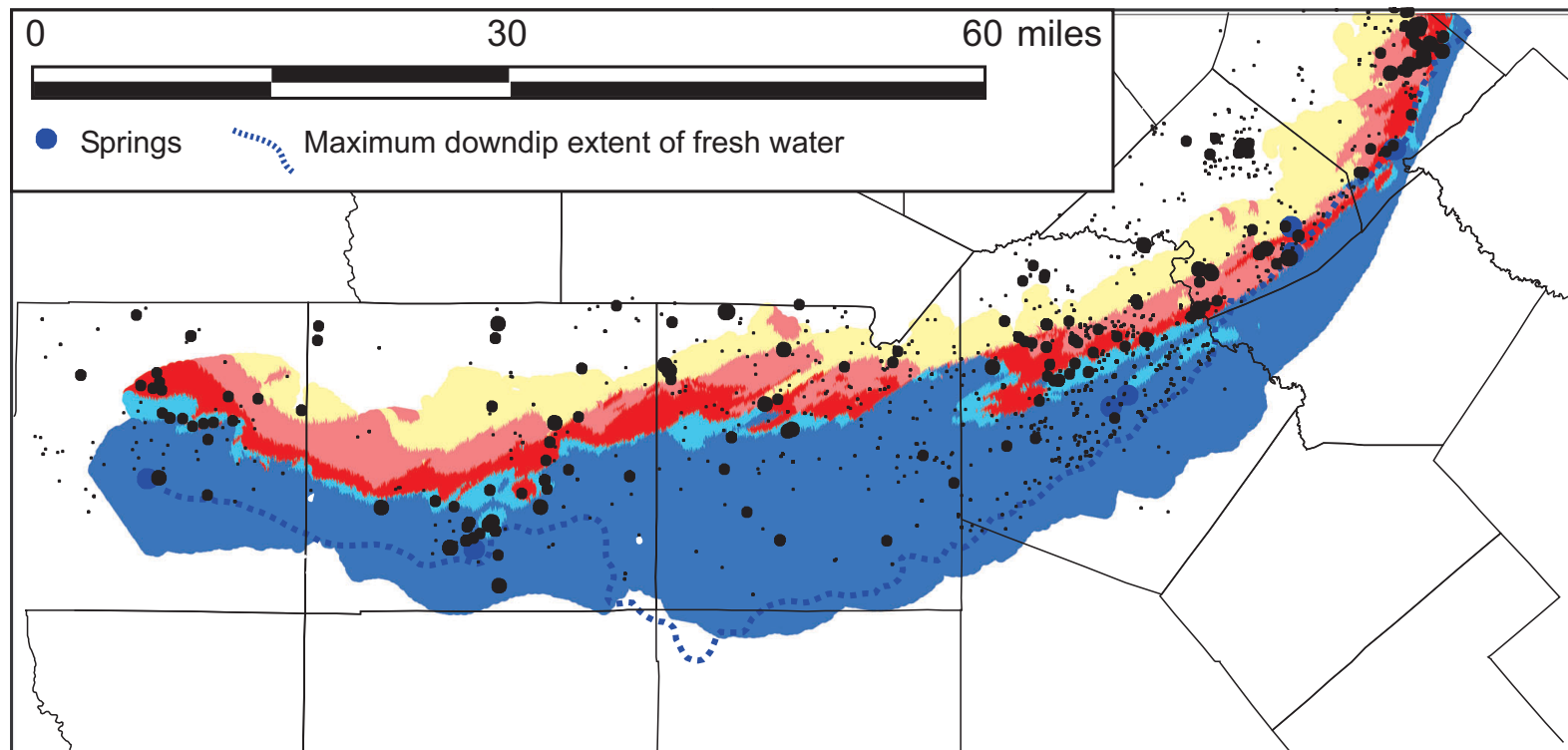


Figure 17. Calcite saturation, from “saturated near 1” to “undersaturation (strongly negative numbers)” plotted on the saturated-thickness base (low-pseudosynoptic water-level map).



Aquifer thickness

- Unsaturated
- Kainer and equivalents saturated
- Person and equivalents saturated
- Saturated thickness 500- to 600 feet
- Edwards Group fully saturated

NO₃ in mg/l

- <30
- 30-300
- >300

Figure 18. NO₃ concentration (ppm) plotted on the saturated-thickness base (low-pseudosynoptic water-level map).

Analysis of hydrographs

We analyzed four well hydrographs with relatively complete records and a clear relationship to a rainfall event. They were matched with rain data from the San Antonio 8 NNE (COOPID# 417947) weather station. Locations of wells analyzed are shown in figure 19.

EAA Well 68-28-202 is an Authority monitoring well north of San Antonio in the recharge zone. Water-level variation is about 10 ft, and recovery is fast, in a few weeks (fig. 20). Two slopes can be clearly distinguished, discriminating between the matrix and fracture-flow components.

EAA well 68-28-519 is located about 1.2 mi southwest of 68-28-202. This well has sharper responses to precipitation pulses, suggesting a larger influence of conduits (fig. 21). Water-level variations are on the order of 15 ft. Storativity of the conduitlike features is about 15% of the fracture system and matrix storativity.

The SAWS Fish Hatchery #1 well (67-09-113) is located in Comal County in the confined section but close to the transition between confined and unconfined. Figure 21 shows the impact of precipitation on well water level. Total agreement does not exist between rain data and water level because of the spatial variability of precipitation during a storm event. Recession due to the first storm has been analyzed. Smaller rain events after the main storm produce multiple peaks. However, water-level decline is not muddled by subsequent storms, as is the second large storm recession curve. Water-level fluctuations are in the range of 10 ft and are displayed in a semilog plot on figure 21b.

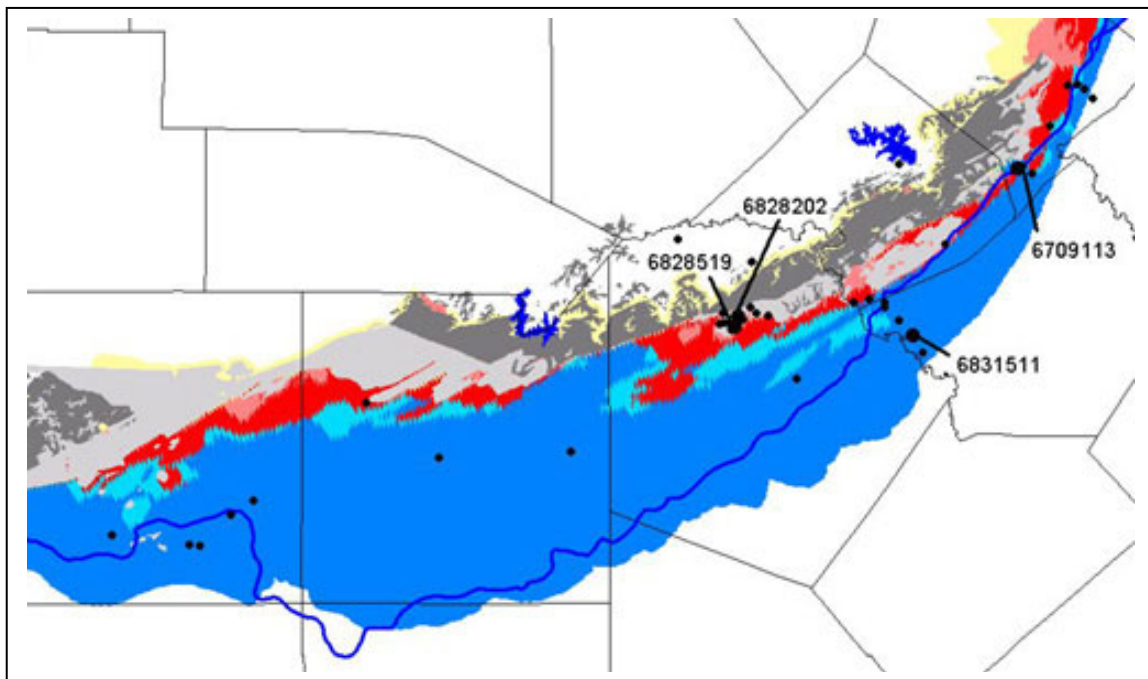


Figure 19. Location of wells selected for hydrograph separation. Other wells equipped with transducers and data loggers, as shown with large dots. However, the high-frequency records obtained for these wells were not suitable for recession analysis during the selected period.

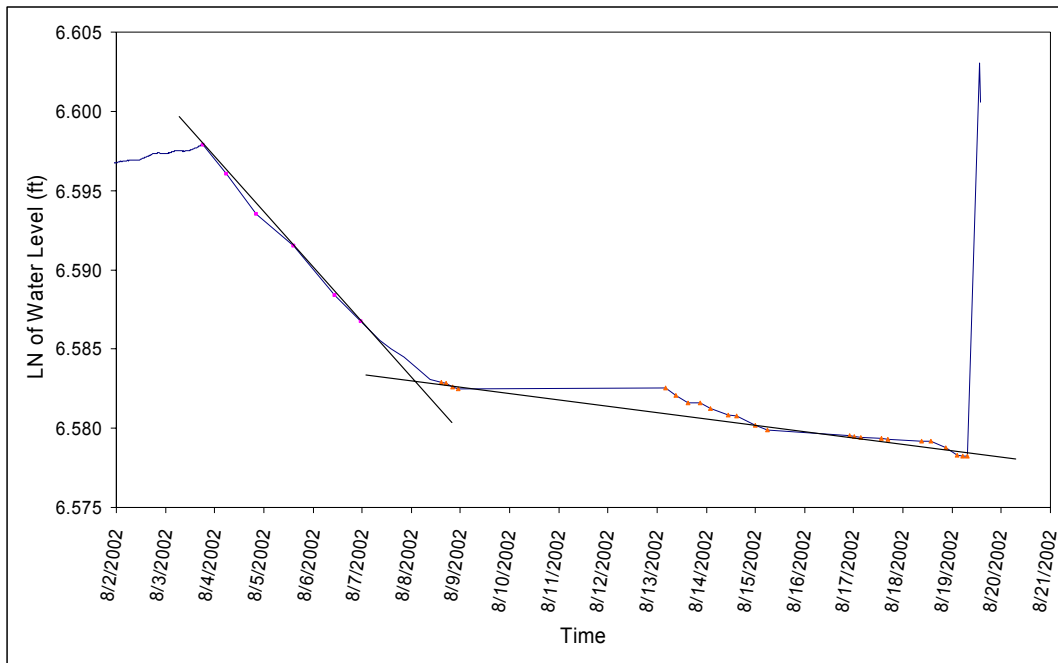


Figure 20. Well hydrograph for 68-28-519.

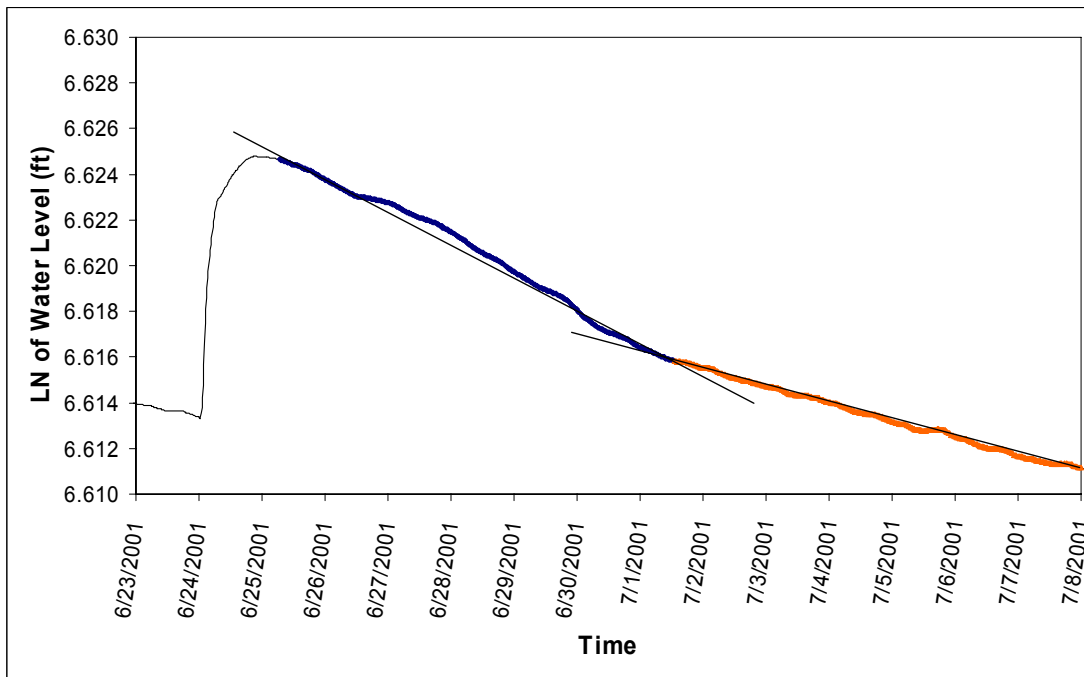
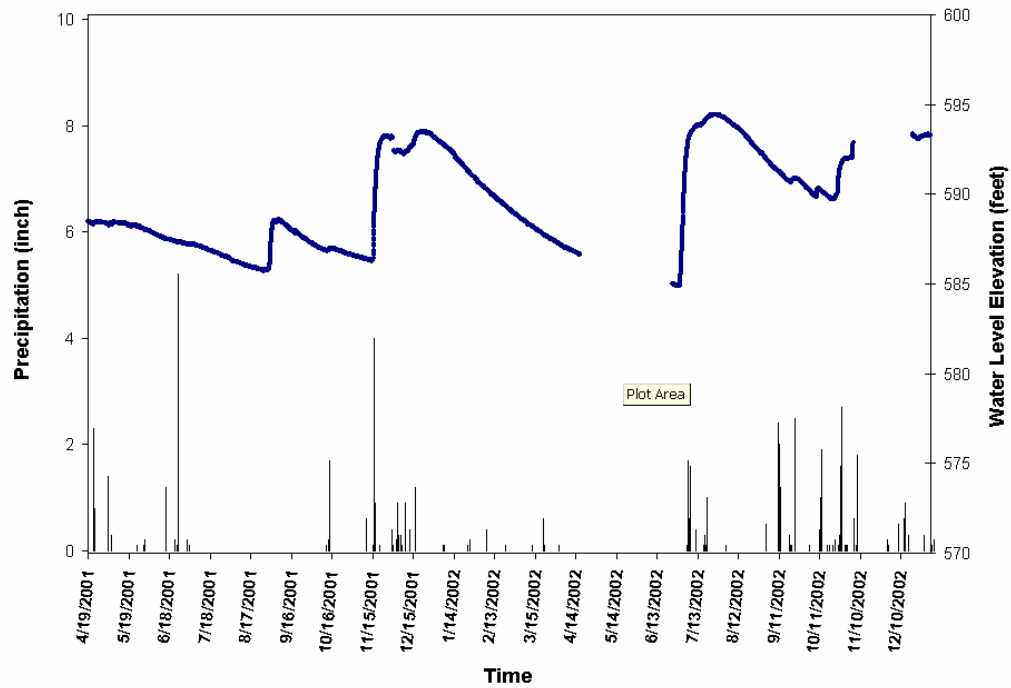


Figure 21. Well hydrograph for 68-28-202.

Water-level decrease is slow, and it takes several months for the well to return to prestorm level. Although there is a clear change of slope, no slope discontinuity is visible, suggesting that there is a porosity continuum in the vicinity of this well. Three or four slope segments can be individualized from figure 21b. They most likely correspond to flow in different fracture groups and in the rock matrix. There is no evidence of an initial, quick water-level decrease generated by the presence of nearby conduits. Application of the method to this well suggests that specific yield of fractures and large connected openings is only two to three times less than the matrix specific yield.

The SAWS Tricounty #3 well is a saline zone well about 5 mi southeast of the fresh-saline interface. Water-level variations are on the order of 10 ft, and recovery is faster than that of 67-09-113 (fig. 22). Two slopes can be distinguished, discriminating between matrix and fracture-flow components. Storativity of the fracture system is about 75% of the matrix storativity. There is no evidence of conduit flow; however, the conduit-flow recession may be hidden because the recharge peak is not sharp.

(a)



(b)

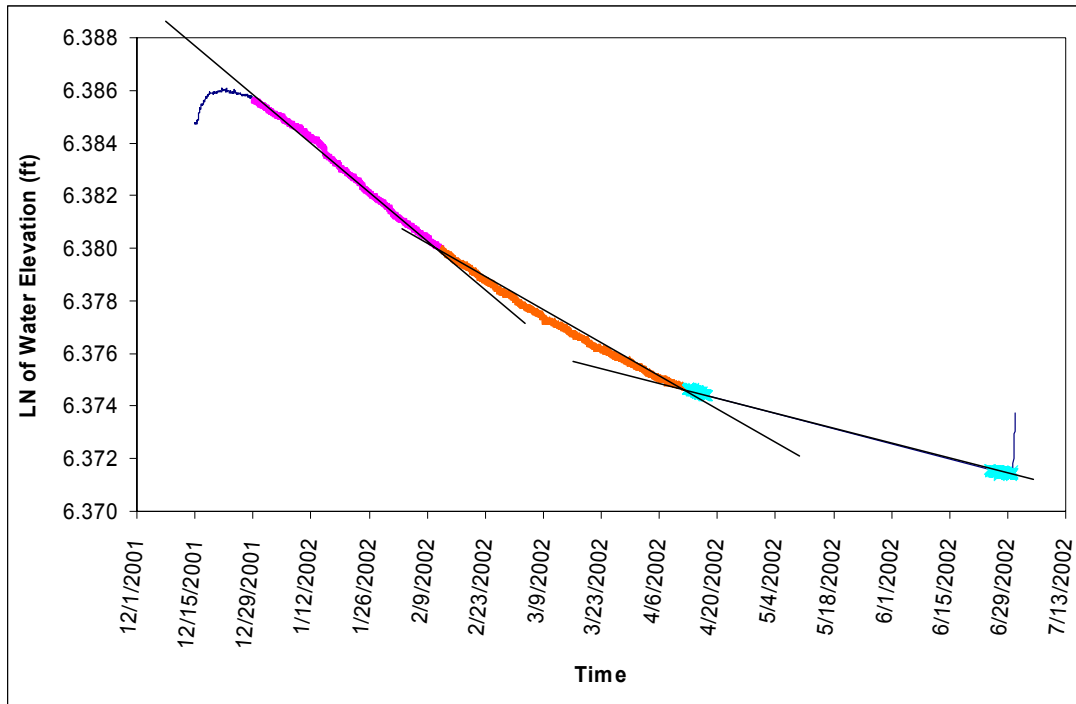


Figure 22. Well hydrograph for the SAWS Fish Hatchery # 1 well, 67-09-113, showing (a) comparison of the hydrograph with several rainfall events and (b) a detailed recession separation.

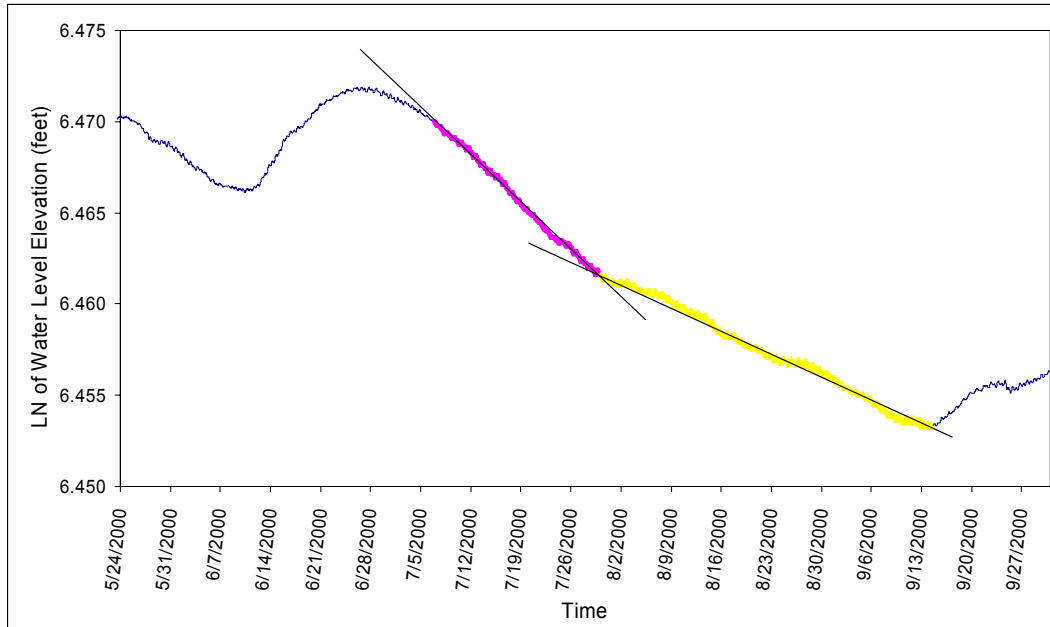


Figure 23. Well hydrograph separation for SAWS Tricounty #3 68-31-511.

DISCUSSION

Integrating and comparing the suite of conduit indicators increase data density, and therefore the potential for better defining of narrow conduit locations (figs. 23, 24). Analog data from other karst systems (for example, Barton Springs Edwards aquifer, fig. 5) show that conduits make up only a small fraction of the rock volume, and the chances of intercepting a conduit with a well are small. In the Edwards aquifer, measurements using several methods show that only about 2% of the rock volume is occupied by centimeter-scale or larger conduits (Hovorka and others, 1998). Large-aperture, interconnected conduits proportionally make up an even smaller proportion of the rock volume. Hydraulic properties show that most wells are not closely connected to large-aperture conduits with turbulent flow (Halihan and others, 2000). However, conduit flow is a critical parameter in aquifer performance, especially aquifer capacity to store water during periods of low recharge. In order to identify, measure, and monitor the conduits, it is important to screen available information for clues as to their distribution and characteristics.

Integrating and classifying historical water levels to create pseudosynoptics provided, at low cost, three or four times the number of data points that are available in the high-quality synoptic surveys coordinated by Authority (Esquilin, digital communication, 2003), leading to better definition of troughs, especially in marginal areas. The subtracted high-low pseudosynoptic (fig. 11) shows the flaws in this system. Trinity water levels do not appear to have responded to the same trends in stage as those

of Edwards wells, as reflected in “high” water levels below “low” water levels for parts of the recharge zone. We have preferentially used the low pseudosynoptic (fig. 23) for interpretation to minimize these errors because recession curves for almost all wells trend downward toward a stable value. High and intermediate pseudosynoptics, as well as the real synoptics, were used to replicate, confirm, and better define trough locations.

Five conduit indicators are considered: troughs, no drawdown wells, low TDS, low calcite saturation, and high nitrate (fig. 24). These indicators are not unequivocal evidence that the well intercepted a conduit because other explanations for the observation are possible. For example, some troughs in the aquifer are likely the result of pumping in a region of the aquifer that is not well connected. No drawdown during specific-capacity testing indicates that hydraulic conductivity of the aquifer was larger than could be tested by the tubing and pump used. Many of these wells were drilled for domestic water supply and well diameter, and pumps were typically small. Mace and Hovorka (2000) calculated a minimum hydraulic conductivity for these wells by assigning an arbitrary, small drawdown. Most of the minimum hydraulic conductivities lie in the range modeled as fracture flow by Halihan and others (2000). However, it is likely that an unknown percentage of no-drawdown wells have hydraulic conductivities much greater than the minimum, indicating that the well bore is hydraulically influenced by a conduit. Likewise, some geochemical conduit indicators may be the result of high vertical transmissivity (leaking well bore), sampling, or analytical error. It is expected that many wells with conduit indicators lie within the region influenced by a conduit but do not penetrate the conduit volume. The size and geometry of this region of influence are not well known but are conceptualized on the basis of outcrop analogs as a network of solution-enlarged fractures and bedding-plane partings that were intercepted by the open hole part of the well and provide good connection in three dimensions to a regionally extensive, pipelike conduit system characterized by turbulent flow.

In overview, pseudosynoptics confirm well-known trends: a broad, low-gradient part of the aquifer in the confined zone, steep gradients between the Edwards and Trinity aquifers, and a steepening of Edwards gradient in eastern Uvalde County (the “Knippa gap” of Maclay) (figs. 7, 8, 9).

Steep gradients between the confined and unconfined Edwards

Looking first at the transition between the confined and unconfined aquifer, we consider the hypothesis of Maclay and Land (1988) that large throw faults segment the aquifer and divert flow entering the recharge zone on relay ramps to the west before it swings back toward the east. Superimposing faults on the low pseudosynoptic (fig. 23) shows several areas of steep gradient coincident with faults, but in most areas the water level appears to be gradational rather than sharp. Small troughs that cross the faults that juxtapose the Glen Rose with the Edwards Formation are poorly defined but appear to be generally perpendicular to the faults. Comparing figures 7, 8, and 9 shows that the area of steep gradient migrates with aquifer stage, and well control is adequate to define a gradational rather than a sharp break.

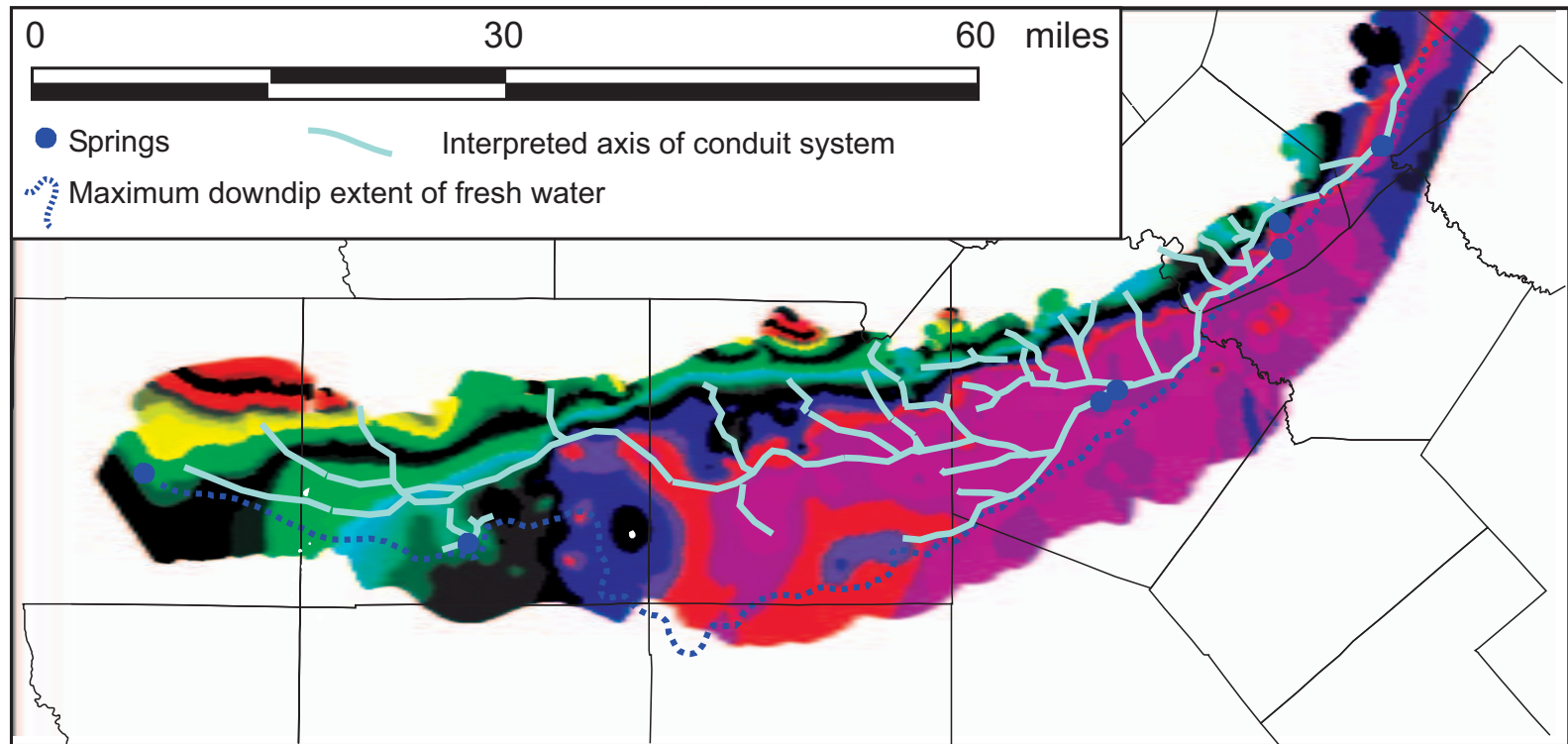
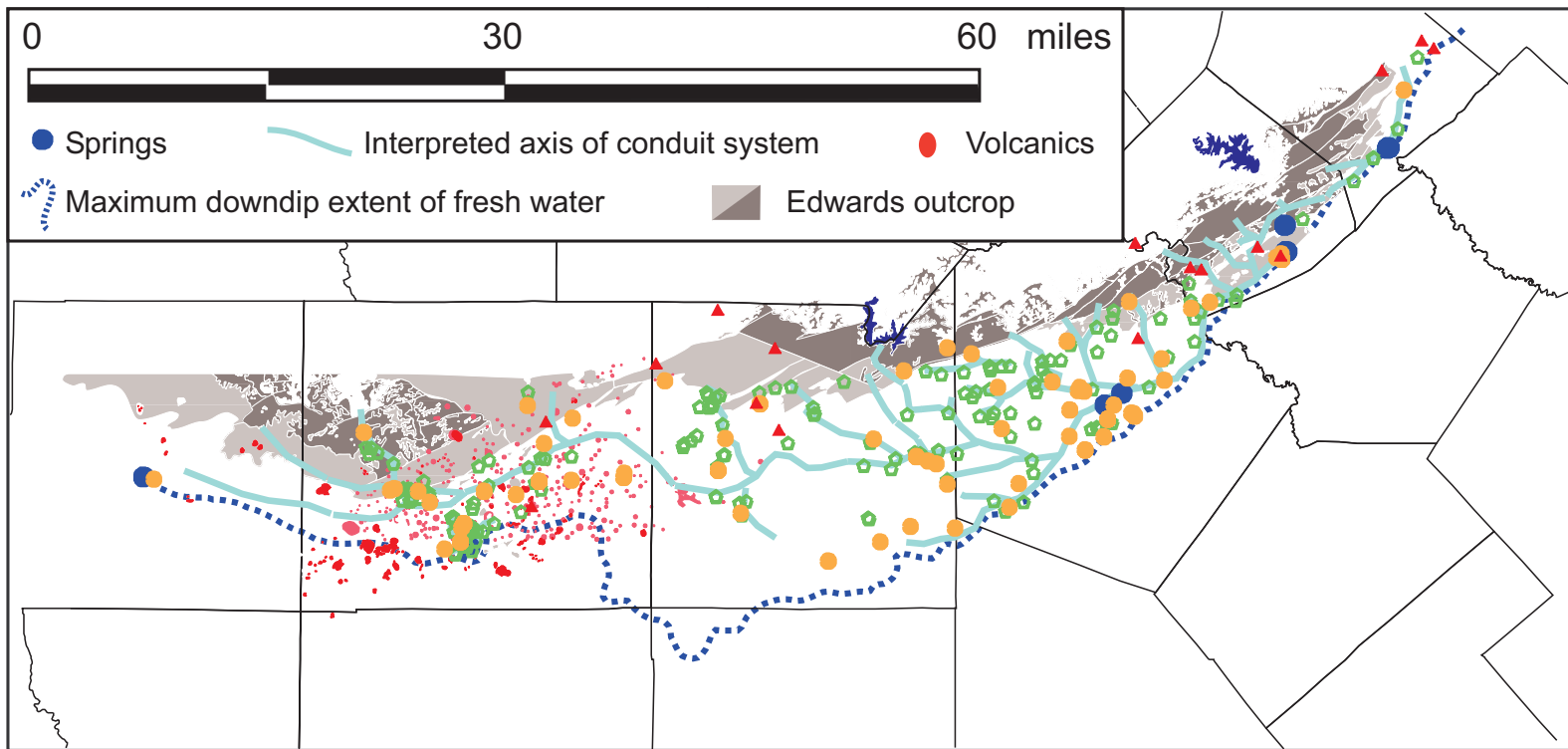


Figure 24. Interpreted low-pseudosynoptic water levels with fault patterns superimposed. Regions of large throw faults that coincide with steep gradients are highlighted by red lines. Pumping centers that form depressions are shown by green circles, and interpreted axes of conduit systems are shown by blue lines.



Conduit indicators

- ◇ No drawdown well
- Calcite undersaturation
- ▲ $\text{NO}_3 > 50 \text{ mpp}$

Figure 25. Conduit indicators and interpreted axes of persistent troughs in the pseudosynoptic potentiometric surface maps.

Because of the steepness of the gradient observed in the Edwards confined section, it does not seem to be controlled exclusively by a change in aquifer properties between the Edwards and the Trinity. Location of the steep gradient best fits the saturated thickness map (fig. 12a). The area of flat gradient fairly closely corresponds to occurrence of a fully saturated Person section. This correspondence may be a function of saturated thickness, intersection of a high permeability zone at the top of the Edwards, or the transition from unconfined to confined aquifer dynamics. The transition from the unconfined to confined Edwards aquifer is not coincident in detail with the outcrop of the Edwards Group. In the eastern and central parts of the outcrop, the Edwards Formation is unsaturated beneath most of the Kainer and lower Devils River outcrop. Beneath the Person outcrop, the Kainer is saturated, and the Person is only partly saturated for the first 1.5 to 4 mi, where the Edwards is overlain by younger rocks that make up the confining units. A generalized cross section of the transition from the unconfined to confined Edwards shows these relationships (fig. 25).

This geometry raises the question: what pathway is taken by water that recharges in the Kainer and lower Devils River outcrop? Veni (written communication, 2003) has documented cave patterns in the Camp Bullis area, as well as other locations in the recharge zone, that indicate that the upper part of the Glen Rose Formation is hydrologically connected to the Edwards Group. Three hypothesis are proposed: (1) recharge moves through the Kainer and into the upper Glen Rose Formation, moves directly down gradient, and then crosses the first fault and reenters the Kainer Formation; (2) recharge moves through the Kainer and into the upper Glen Rose Formation; however, the fault is a barrier and flow must move laterally through an undefined

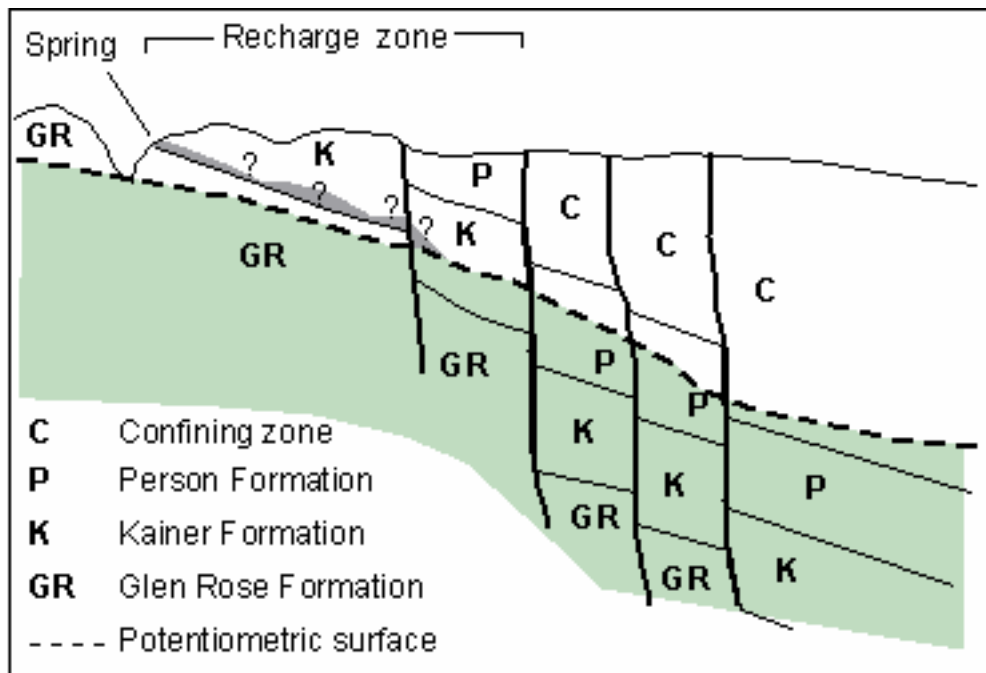


Fig 26. Schematic cross section of the transition from the unconfined to confined Edwards in the eastern and central parts of the aquifer.

pathway before it encounters a gap and reenters the Kainer Formation; or (3) recharge entering the Kainer Formation is perched on the lower permeability units at the Glen Rose contact and moves laterally through the Kainer Formation an unknown distance before it finds a break and can move into either the Edwards or the Glen Rose Formation. The process hypothesized in 3 may occur only during active recharge, in which case the water would be transmitted rapidly through conduit flowpaths.

The potentiometric surfaces mapped support hypothesis 1 as a regional model. Water levels are steep but continuous and move in response to stage change across the transition from the unconfined to confined Edwards. The steepness of the gradient suggests that transmissivity is low, which may mean that hypothesis 2 is active on a fine scale and that cross-fault flow is limited by rock properties along the faults. Partial saturation may also have a role, for example, if the highest permeability is found at the top of the Edwards Group associated with the paleokarst surface. Numerous small springs discharge toward the north along the updip Edwards-Glen Rose contact in outcrop (figs. 3, 25), which supports hypothesis 3. However, we have no evidence of perched conduits in the Edwards recharge zone. Perched conduits have been documented in other cave systems and might be active in areas not penetrated by wells—for example, beneath rivers. Conduits serving as an intermittent high-stage flow system would be difficult to intersect with wells, but if such a system is operative, it has important implications for storage and transport.

Only at large throw faults, such as the one at the Bexar-Medina County line and the one in eastern Uvalde County (red bars, fig. 23), is there a transition directly from Edwards outcrop to confined Edwards aquifer across a fault boundary. In the western area, the change from unconfined to confined Edwards is more transitional. The Edwards section is partly saturated even beneath outcrop of the Kainer-equivalent West Nueces and McKnight Formations, and the Person-equivalent Salmon Peak Formation is partly unsaturated almost as far south as the fresh-saline interface.

Trends and variations in the unconfined Edwards

In overview, pseudosynoptic water-level maps confirm well-known trends: steep gradients between the Edwards and Trinity aquifers and a steepening of the Edwards gradient in eastern Uvalde County (the “Knippa gap”). On top of these general trends, increased data density defined a number of smaller features. In order to confirm and refine the distribution of conduits, we posted other potential conduit indicators: no-drawdown wells, calcite undersaturated and low TDS waters, and high nitrate (fig. 24). In mapping conduits, we considered the findings from the cave-orientation survey, which revealed that about half of horizontally elongated caves are elongated along the major opening-mode fracture trend parallel to the extensional faults; in the other half, gradient or diversely oriented fracture trends are controls.

Moving across the aquifer from east to west, we considered indications of observed relationships. The lowest point in the aquifer near San Marcos Springs is a small depression that is not well defined by available data. A recurrent low point

(values lower than spring level) in the pseudosynoptic occurs north of San Marcos Springs (fig. 23, green circle). It is interpreted as a response to a pumping center at Kyle and not a conduit indicator. This trough at a pumping center is likely an indicator of relative hydrologic isolation of the area because of poor karst connectivity near the groundwater divide between south-central and the Barton Springs segments. Only a narrow zone within the graben is fully saturated, and it contains several no-drawdown wells and several wells that plot as calcite undersaturated. This situation is interpreted to be a likely location of a conduit. Historical data density in the southern Hays County area is inadequate for examining cross-formational flow, although San Marcos Springs is interpreted to receive significant local recharge (Ogden and others, 1986).

The pseudosynoptic water-level map is somewhat useful in refining the poorly understood connection between San Marcos Springs and the rest of the aquifer. The freshwater aquifer in the confined section is extremely narrow or even nonexistent in sections between San Marcos and Comal Springs (fig. 23). Large throw faults in this area displace the Edwards Group, so that at the bad-water line, Edwards blocks are not in contact. Several workers (S. Worthington, 2002, written communication) have hypothesized that rather than flowing through the confined section, significant flow moves through the large graben system within the Edwards outcrop in southern Comal County. Data density in the pseudosynoptic water-level map is much higher in this area than that of real synoptic water-level measurements; however, well spacing is inadequate to resolve any troughs associated with the graben. Several calcite-undersaturated water samples provide support for this model. This graben preserves post-Edwards rocks in outcrop, but the Edwards is only partly saturated. Note that in the model for evolution of the Edwards aquifer by karst capture (Woodruff and Abbot, 1986), it may be a zone of relatively recent integration, and conduit systems may be in development.

Between Comal Springs and eastern Bexar County, the pseudosynoptic water-level map defines a trough or half-trough coincident with multiple no-drawdown wells and calcite-undersaturated wells mostly within 1 mi or less of the mapped bad-water line. This conduit flows parallel to major faults near Comal Springs but moves across faults at a high angle to occur deeper in the subsurface in Bexar County (fig. 23). An area of higher pressure is defined by water levels in parts of the saline zone in Guadalupe County. Several poorly defined conduits are interpreted to connect this master conduit with the recharge zone. Several high-nitrate samples are used to suggest locations of these systems (fig. 24).

In the north and east parts of the confined aquifer, water levels over broad areas of the aquifer are nearly flat. The well-known trough from central Bexar County to western Medina County is clearly apparent. The 6- to 10-mi width defined by high well density and numerous no-drawdown, calcite-undersaturated, and low-TDS wells suggests that the trough is formed by a complex of interconnected conduits. The east-west trend of the entire system suggests a structural influence. In detail, about half the segments are fault parallel, and half of them cross faults at a significant angle. A half-trough is partly defined by gradients toward the bad-water line and is associated with several no-drawdown wells. West of eastern Medina County, well density is inadequate to trace this deep conduit farther. Several 3- to 7-mi-long sections of large throw faults are coincident with a steep gradient between confined and unconfined sections. This fact suggests that

faults or stratigraphic juxtaposition limit cross-fault flow; however, notches in the pseudosynoptic water-level map suggest that more transmissive zones provide connection between the recharge zone and the confined aquifer. Notches are mapped as inferred conduit axes, although the steep gradient demonstrates that flow properties of these systems are different from those of the confined zone. Several hydrographs near one of the inferred conduit axes were analyzed (figs. 20, 21) but do not separate to show distinctive conduit properties.

Pseudosynoptic water-level maps define a continuation of a prominent trough that swings northward around the volcanic center in southeastern Uvalde County. High water-level variability (fig. 11) in western Medina County shows that the zone that stores water occurs over a fairly broad area generally coinciding with the Devils River Trend (fig. 1). This area is characterized by a thick, relatively homogeneous section dominated by grain-rich limestone. It may represent a maximum in matrix storativity because of high porosity but a minimum in solution enlargement of conduits because dolomite is a minor phase with the rock.

Pseudosynoptic water-level maps show a complex pattern in central Uvalde County, probably reflecting rock complexity in this area with complex structural and volcanic intrusions. No-drawdown wells occur in disproportionate numbers near Leona Springs and along a zone trending northwest from them. Details of the connectivity of flow through this area are unclear; however, a network of conduits is inferred from available data. Increased saturated thickness of the Edwards section in the western area in the West Nueces, McKnight, and Salmon Peak Formations may be related to different rock properties of the Maverick Basin (fig. 1). Because of the basinal depositional environment, these rocks have been less strongly modified by dolomitization and dissolution than the platformal rocks of the Kainer and Person Formations (Hovorka and others, 1998). We hypothesize that the ratio of storage in matrix to storage in fractures and conduits may be higher in the west than in the more strongly karst modified eastern area. Several low areas are found in southeastern Uvalde County. These areas may be cones of depression near pumping centers in a low-transmissivity region. Alternatively, these depressions could be the expression of the west end of a conduit developed along the bad-water line.

Subtle troughs suggest that focused flow processes are active into Kinney County. Numerous calcite-undersaturated water samples are found in both the unconfined and confined aquifer in this area.

Follow-up recommendations

One main purpose of this study is to define areas and methods for future field work. We posted known well locations on the descriptions developed above to identify some areas that could be tested to confirm or modify the conclusions of this study (fig. 26). We propose that focused studies on a selection of the areas in red boxes might include (1) a real synoptic water-level survey at low aquifer stage; (2) water chemistry sampling to measure calcite saturation and salinity, including some high-frequency conductivity measurements across several recharge events; (3) recording high-frequency water level, temperature, and conductivity measurements along a transect across several recharge events.

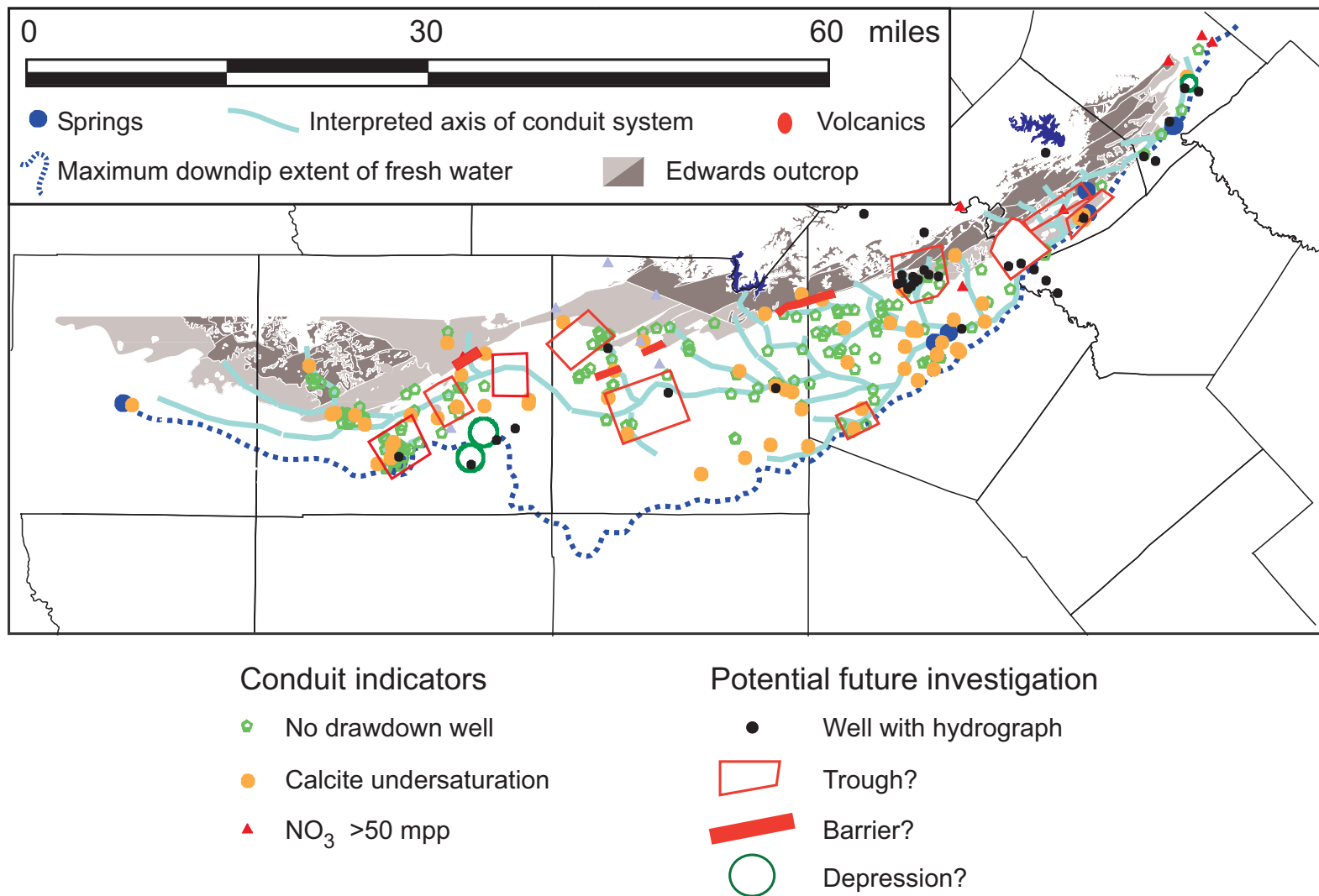


Figure 27. Suggested detailed study areas.

The hydrograph separation method has the potential to assess the location and properties of conduits. This approach will help in determining properties of those wells not responsive to pump testing because they show no drawdown. They, however, should be responsive to large-scale stresses brought to the aquifer by storm recharge events. As more high-quality, high-frequency (15-minute), water-level records are collected, it will be possible to analyze more of them from existing monitored wells. Increased temporal resolution of pumping and rainfall distribution now being collected will improve analysis of these records also.

Coupled with these tests, which use the natural aquifer response for tracing flow, is the possibility of intercepting introduced tracers. In all but the test areas near the springs, wells within the conduit system will be needed to intercept the introduced tracer. Natural tracers are proposed as a method for identifying wells that can be used for these intercepts.

ACKNOWLEDGMENTS

This analysis is built entirely on the labor of others, who for decades have collected a monumental volume of data from the Edwards aquifer. We thank Geary Schindel, Steve Johnson, John Hoyt, Rob Esquilin, and Nedco Troshanov of the Edwards Aquifer Authority for their help in compiling recent and historic data from paper and digital records. John Waugh and Denise Reneghan of the San Antonio Water System and Eric Strom and the GIS group at USGS provided high-frequency water records. Nico Hauwert from the City of Austin and Brian Smith from the Barton Springs Edwards Aquifer Conservation District supplied data and advice. We thank Jerry Fant, Jim Kennedy, and George Veni for providing access to Texas Speleological Society archives and databases. We thank our colleagues at the Bureau, Joseph Yeh, Alan Dutton, Bridget Scanlon, John Andrews, and Becky Smith for a wide variety of assistance throughout this project from digital data handling to insights into aquifer processes. Steve Worthington provided valuable interim review comments.

REFERENCES CITED

- Barton Springs/Edwards Aquifer Conservation District, 2003, Summary of groundwater dye tracing studies (1996-2002), Barton Springs segment of the Edwards Aquifer; fact sheet Barton Springs/Edwards Aquifer Conservation District
- Clark, A. K., 2000, Vulnerability of ground water to contamination, Edwards Aquifer recharge zone, Bexar County, Texas, 1998: U.S. Geological Survey Water Resources Investigations Report 00-4149.
- Deike, R. G., 1990, Dolomite dissolution rates and possible Holocene dedolomitization of water-bearing units in the Edwards aquifer, south-central Texas: *Journal of Hydrology*, v. 112, no. 3-4, p. 335-373.
- Elliott, W. R., and Veni, George, eds., 1994, The caves and karst of Texas; Guidebook for the 1994 convention of the National Speleological Society with emphasis on the southwestern Edwards Plateau: National Speleological Society, Huntsville, AL, 342 p.
- Ferrill, D. A., and Morris, A. P., 2003, Dilatational normal faults: *Journal of Structural Geology*, v. 25, p. 183-196.
- Groschen, G. E., and Buszka, Paul, M., 1997, Hydrogeologic framework and geochemistry of the Edwards aquifer saline-water zone, south-central Texas: U.S. Geological Survey Water-Resources Investigations Report 974133.
- Halihan, Todd, Mace, R. E., and Sharp, J. M., 2000, Flow in the San Antonio segment of the Edwards aquifer; matrix, fractures, or conduits? *in* Sasowsky, I. D., and Wicks, C. M., Groundwater flow and contaminant transport in carbonate aquifers: Brookfield, Vermont, A. A. Balkema, p. 129-146.
- Hauwert, N. M., Sansom, J. W., Jr., Johns, D. A., and Aley, T. A., 2002, Groundwater tracing study of the Barton Springs segment of the Edwards aquifer, Southern Travis and northern Hays Counties, Texas: Barton Springs/ Edwards Aquifer Conservation District and City of Austin Watershed Protection Department.
- Hovorka, S. D., Dutton, A. R., Ruppel, S. C., and Yeh, J. S., 1996, Edwards aquifer ground-water resources: geologic controls on porosity development in platform carbonates, South Texas: The University of Texas at Austin, Bureau of Economic Geology Report of Investigations No. 238, 75 p.
- Hovorka, S. D., and Mace, R. E., 1997, Interplay of karst, fractures, and permeability in the Cretaceous Edwards aquifer: analogs for fractured carbonate reservoirs: Society of Petroleum Engineers Annual Conference and Exhibition, Geological Field Trip Guidebook, 35 p.
- Hovorka, S. D., Mace, R. E., and Collins, E. W., 1998, Permeability structure of the Edwards Aquifer, south Texas—implications for aquifer management: The University of Texas at Austin, Bureau of Economic Geology Report of Investigations No. 250, 55 p.

- Johnson, S. B., Schindel, G. M., and Hoyt, J. R., 2002, Groundwater chemistry changes during a recharge event in the karstic Edwards Aquifer, San Antonio, Texas: Geological Society of America, Online Abstract 186-8.
- Klemt, W. B., Knowles, T. R., Edler, G. R., and Sieh, T. W., 1979. Ground-water resources and model applications for the Edwards (Balcones Fault Zone) aquifer in the San Antonio Region: Texas Water Development Board Report No. 239.
- Klimchouk, A. B., Ford, D. C., Palmer, A. N., and Dreybrodt, Wolfgang, eds., 2000, Speleogenesis—evolution of karst aquifers: National Speleological Society, Huntsville, Alabama, 527 p.
- Krejca, J. K., 2002, Genetic relatedness of aquifer organisms as a tool for determining aquifer connectedness, *in* Martin, J. B., Wicks, C. M. and Sasowsky, I. D., eds. Hydrogeology and biology of post-Paleozoic carbonate aquifers: Proceedings of the Symposium on Karst Frontiers: Florida and related environments, March 6–10, Gainesville, Florida: Special Publication 7 of the Karst Waters Institute, Charlestown, West Virginia, p 157-161.
- Land, L. S., and Prezbindowski, D. R., 1981, The origin and evolution of saline formation water, Lower Cretaceous sediments, south-central Texas, U.S.A., *in* Back, W., and Letolle, R., Symposium on Ground Water Hydrology: Journal of Hydrology, v. 54, 51-74.
- Lindgran, R. J., Dutton, A. R, and Hovorka, S. D, in preparation, Conceptualization and simulation of the Edwards Aquifer, San Antonio Region, Texas: Contract report to the Edwards Aquifer Authority
- Longley, Glen, 1986, The biota of the Edwards aquifer and the implications for biozoogeography, *in* Abbott, P. L. and Woodruff, C. M., Jr., eds., The Balcones Escarpment, Central Texas: Geological Society of America, p. 51-54: <http://www.lib.utexas.edu/geo/BalconesEscarpment/pages51-54.html>
- Mace, R. E., Fisher, R. S., Welch, D. M., and Parra S. P., 1997, Extent, mass, and duration of hydrocarbon plumes from leaking petroleum storage tank sites in Texas: The University of Texas at Austin, Bureau of Economic Geology Geological Circular 01, 52 p.
- Mace, R. E., and Hovorka, S. D., 2000, Estimating porosity and permeability in a karstic aquifer using core plugs, well tests, and outcrop measurements, *in* Sasowsky, I. D., and Wicks, C. M., Groundwater flow and contaminant transport in carbonate aquifers: Brookfield, Vermont, A. A. Balkema, p. 93-111.
- Maclay, R. W., 1995, Geology and hydrology of the Edwards Aquifer in the San Antonio area, Texas: U. S. Geological Survey Water-Resources Investigation report 95-4186, 64 p.
- Maclay, R. W., and Land, L. F., 1988, Simulation of flow in the Edwards aquifer, San Antonio Region, Texas, and refinements of storage and flow concepts: U.S. Geological Survey Report Water-Supply Paper 2336, 48 p.

- Ogden, A. E., Quick, R. A., Rothermel, S. R., and Lundsford, D. L., 1986, Hydrological and hydrochemical investigation of the Edwards aquifer in the San Marcos area, Hays County, Texas: Edwards Aquifer Research and Data Center, San Marcos, Texas, 364 p.
- Painter, Scott, Jiang, Yefang and Woodbury, Allan, 2002, Edwards aquifer parameter estimation project final report: Southwest Research Institute, variably paginated.
- Palmer, A. N., 1991, Origin and morphology of limestone caves: Geological Society of America Bulletin, v. 103, p. 1-21.
- Powers, J. J. and Shevenell, Lisa, 1999, Transmissivity estimates from well hydrographs in karst and fractured aquifers: Ground Water, v. 38 no. 3, p. 361-369.
- Rettman, P. L., 1991, Worlds largest flowing well: Twichell hydrology symposium: American Water Resources Association, Texas Section, Fort Worth, TX, p. 64
- Rorabaugh, M. I., 1964, Changes in bank storage: Publ. No.63, IASH, Gentbrugge, p. 432-441.
- Rose, P. R., 1972, Edwards Group, surface and subsurface, Central Texas, The University of Texas at Austin, Bureau of Economic Geology Report of Investigations 74, 198 p.
- Russell, William, Loder, Wess, and Sprouse, Peter, 1974, Airmans cave, Travis County: unpublished map from Texas Speleological Society archives.
- Scanlon, B. R., Mace, R. E., Smith, Brian, Hovorka, Susan, Dutton, A. R., and Reedy, Robert, 2001, Groundwater availability in the Barton Springs segment of the Edwards aquifer, Texas: numerical simulation through 2050: The University of Texas at Austin, Bureau of Economic Geology open file report http://www.beg.utexas.edu/enviro/qly/vadose/pdfs/webbio_pdfs/BartonSpringsFinalReportFeb2002.pdf, 99 p.
- Schindel, G. M., Johnson, S. B., Worthington, S. R. H., Alexander, E. C., Jr., Alexander, Scott, and Schnitz, Lewis, 2002, Groundwater chemistry changes during a recharge event in the karstic Edwards Aquifer, San Antonio, TX, Geologica Society of America Abstracts with Program http://gsa.confex.com/gsa/2002AM/finalprogram/abstract_44210.htm
- Schultz, A. L., 1992, Using geophysical logs in the Edwards aquifer to estimate water quality along the freshwater/saline-water interface (Uvalde to San Antonio, Texas): Edwards Underground Water District Report 92-03, 47 p.
- Schultz, A. L., 1993, Defining the Edwards aquifer freshwater/saline-water interface with geophysical logs and measured data (San Antonio to Kyle, Texas): Edwards Underground Water District Report 93-06, San Antonio, Texas, 81 p.
- Schultz, A. L., 1994, 1994 review and update of the position of the Edwards aquifer freshwater/saline-water interface from Uvalde to Kyle, Texas: Edwards Underground Water District report 94-05, 31 p.

- Shevenell, Lisa, 1996. Analysis of well hydrographs in a karst aquifer: estimates of specific yields and continuum transmissivities: *Journal of Hydrology*, v. 174, p. 331-355.
- Smith, D. V., Smith, B. D. Blome, C. D., Pierce, H. A., and Lambert R. B, 2002, Cretaceous volcanic intrusives in the Edwards aquifer, Texas, as identified from a high-resolution aeromagnetic survey, http://txwww.cr.usgs.gov/aquifer/GSAposter_9NEW.pdf
- Tomasko, David, Fisher, Ann-Marie, Williams, G. P, and Pentecost, E. D, 2001, A statistical study of the hydrologic characteristics of the Edwards aquifer: Argonne National Labs final contract report, on CD.
- Veni, George, 1988, The caves of Bexar County, second edition: The University of Texas at Austin, Texas Memorial Museum Speleological Monograph 2, 300 p.
- Wermund, E. G., Cepeda, J. C., and Luttrell, P. E., 1978, Regional distribution of fractures in the southern Edwards Plateau and their relationship to tectonics and caves: The University of Texas at Austin, Bureau of Economic Geology Geological Circular 78-2, 14 p.
- White, W. B., and White, E. L., 1989, Karst hydrology: concepts from the Mammoth Cave area: Van Nostrand Reinhold, New York, 346 p.
- Woodruff, C. M., and Abbott, P. L., 1986, Stream piracy and evolution of the Edwards Aquifer along the Balcones Escarpment, Central Texas, *in* Abbot, P. L., and Woodruff, C. M., Jr. eds., The Balcones Escarpment, central Texas: Geological Society of America Annual Meeting, p. 77-100.
- Worthington, S. R.H., in prep, Conduits and turbulent flow in the Edwards Aquifer, Worthington Groundwater, contract report to Edwards Aquifer Authority.
- Young, Keith, 1977, Middle Cretaceous rocks of Mexico and Texas, *in* Bebout, D. G., and Loucks, R. G., eds., Cretaceous carbonates of Texas and Mexico: The University of Texas at Austin, Bureau of Economic Geology Report of Investigations No. 89, p. 325-332.